

Dynamics of Pseudoentanglement

Xiaozhou Feng and Matteo Ippoliti

Department of Physics, The University of Texas at Austin, Austin, TX 78712, USA

The dynamics of quantum entanglement plays a central role in explaining the emergence of thermal equilibrium in isolated many-body systems. However, entanglement is notoriously hard to measure, and can in fact be “forged”: recent works have introduced a notion of *pseudoentanglement* describing ensembles of many-body states that, while only weakly entangled, cannot be efficiently distinguished from states with much higher entanglement, such as random states in the Hilbert space. In this work we initiate the study of the dynamical generation and propagation of pseudoentanglement. As generic quantum dynamics tends to maximize actual entanglement, we consider constrained models of time evolution: *automaton* (i.e. reversible classical) circuits that, when fed suitable input states, provably produce the “standard models” of pseudoentangled ensembles—uniformly random *subset-phase states* and *subset states*—at late times, a phenomenon we name *pseudothermalization*. We examine (i) how a pseudoentangled (random subset-phase) ensemble on a small subsystem spreads to the whole system as a function of time, and (ii) how a pseudoentangled (random subset) ensemble is generated from an initial product state. We map the above problems onto a family of classical Markov chains on subsets of the computational basis. The mixing times of such Markov chains are related to the time scales at which the states produced from the dynamics become indistinguishable from Haar-random states at the level of each statistical moment (or number of copies). Based on a combination of rigorous bounds and conjectures supported by numerics, we argue that each Markov chain’s relaxation time and mixing time have different asymptotic behavior in the limit of large system size. This is a necessary condition for a *cutoff phenomenon*: an abrupt dynamical transition to equilibrium. We thus conjecture that our random circuits give rise to asymptotically sharp pseudothermalization transitions.

CONTENTS

		1. Single particle	22
		2. Many particles: multipole eigenmodes	22
		3. Two particles: relative coordinate eigenmodes	23
I. Introduction.	1		
II. Review of key concepts	3		
A. Pseudoentanglement	3	E. Properties of the local automaton gate set	24
B. Equilibration of Markov chains and cut-off phenomenon	4	F. Upper bound on relaxation time with local gate set	25
C. Random walks on permutation groups	5	G. Upper bound on pseudothermalization time for subset states	26
III. Pseudothermalization in automaton circuits	5		
IV. Spreading of Pseudoentanglement	7		
A. Motivation and setup	7		
B. All-to-all circuit model	8		
C. Local circuit model	9		
V. Generation of Pseudoentanglement	13		
VI. Discussion	15		
A. Summary	15		
B. Outlook	15		
Acknowledgments	16		
References	16		
A. Proof of Proposition 1	19		
B. Properties of the Φ maps	20		
C. Proof of Proposition 2	21		
D. Random walk on the hypercube	22		

I. INTRODUCTION.

Entanglement is a fundamental concept in quantum information science and in quantum many-body physics, being both a necessary resource for quantum advantage in information processing [1, 2] and a framework to characterize different phases of matter beyond conventional order parameters [3–5]. Furthermore, the generation and propagation of entanglement in many-body systems is a key ingredient in our understanding of how thermal equilibrium emerges from the otherwise reversible unitary dynamics of isolated systems [6–9]. Due to entanglement, local subsystems may be described by mixed states even when the global state is pure. Such local mixed states can approach universal forms at late times in generic dynamics—namely the Gibbs ensemble $\rho_{A,\text{th}} \propto \text{Tr}_{\bar{A}}(e^{-\beta H})$ [10] and its generalizations [11]—thus recovering predictions of thermodynamics. In the absence of any conservation laws (e.g. in driven systems without

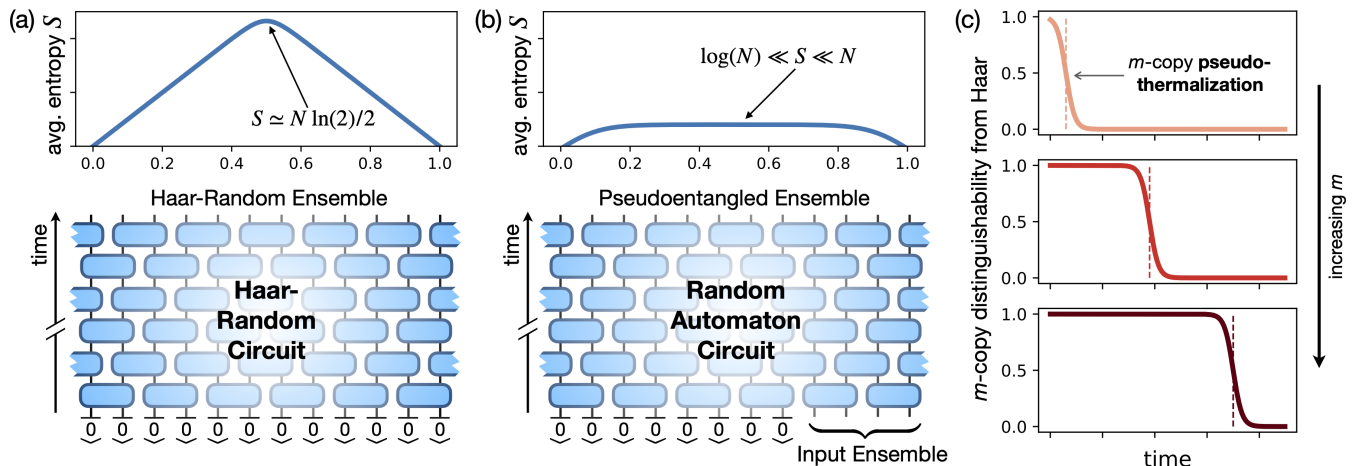


FIG. 1. Main ideas of this work. (a) Quantum thermalization: chaotic quantum dynamics on an isolated many-body systems (modeled by a Haar-random unitary circuit, bottom) produces random states at late times, with near-maximal entanglement entropy described by the Page curve (top). (b) In analogy with thermalization, we consider families of random ‘automaton’ circuits (bottom, see text) that, acting on suitable ensembles of initial states, produce *pseudoentangled* state ensembles at late times. These have relatively low entanglement entropy (top), but are computationally indistinguishable from Page states. (c) We study the dynamical process by which pseudoentanglement is generated and/or propagated over time, quantified by the distinguishability of the output state ensembles from the Haar ensemble: can an observer, by making joint measurements on m copies of an output state, *efficiently* tell it apart from a random state? For each value of m , this defines a time scale dubbed (m -copy) *pseudothermalization time* (vertical dashed lines). This time scale may become sharp in the thermodynamic limit if the problem features a cutoff phenomenon.

symmetries) the predicted late-time equilibrium state for each local subsystem is maximally mixed: $\rho_{A,\text{th}} \propto \mathbb{1}_A$. This requires each local subsystem to become maximally entangled with the remainder of the system. More specifically, in systems modeled by random unitary circuits [12–18] (and even in some quasi-periodically driven systems [19, 20]) one can show that the global pure state of the system resembles a typical Haar-random state in the Hilbert space, also known as a Page state, with a characteristic scaling of entanglement known as the Page curve [21], sketched in Fig. 1(a).

Despite its ubiquity and far-reaching importance, entanglement is generally difficult to control, quantify, and measure [1], especially beyond few-body settings [22]. The last decade has seen substantial progress in these directions, particularly thanks to experimental advances in quantum simulators and theoretical developments in randomized measurements [8, 23–27]; nonetheless, the cost of measuring the entanglement entropy of an N -qubit system remains exponential in N , ultimately limiting the reach of all these approaches.

Recent works [28, 29] highlight the intrinsic subtlety of measuring entanglement in a dramatic way, by introducing a notion of *pseudoentanglement*—a forgery of entanglement that cannot be efficiently distinguished from the real thing. More specifically, they construct ensembles of quantum states that, while only weakly entangled, are indistinguishable from Page states to any observer with a polynomial amount of resources. These ensembles are interesting from the point of view of computation and cryptography [30, 31], and can be efficiently constructed

through the use of quantum-secure pseudorandom permutations [28, 32].

Motivated by the role of entanglement in quantum thermalization, in this work we consider the dynamical generation and propagation of pseudoentanglement in many-body systems. Clearly, to avert the generic tendency of interacting many-body systems to maximize entanglement, we must specialize to non-generic models of time evolution; however, within these constraints (to be discussed below), we introduce random circuit models that prepare pseudoentangled state ensembles as their equilibrium steady states, much like the Page states for generic quantum dynamics. This is sketched in Fig. 1(b). We name this dynamical approach to pseudoentangled ensembles *pseudothermalization*. Depending on one’s perspective, this may be viewed as either a spoofing of quantum thermalization that is practically indistinguishable from the genuine phenomenon, or as a perfectly valid instance of quantum thermalization based on an operational definition (i.e., if a deviation from thermal equilibrium cannot be *efficiently* detected, one may argue it does not count).

Specifically, we consider the random *subset-phase state* ensemble [28] and the random *subset state* ensemble [29], which are fixed points of ‘automaton’ quantum circuits [33–36] (i.e., permutations of the computational basis, not to be confused with ‘quantum cellular automata’). We therefore introduce families of automaton circuits and study the convergence of certain non-equilibrium initial states to these equilibrium fixed points, i.e., the phenomenon of pseudothermaliza-

tion. We focus on two scenarios modeled after paradigmatic problems in ‘true’ quantum thermalization: (i) the spreading of pseudoentanglement from a small subsystem placed in contact with a larger, disentangled system, and (ii) the generation of pseudoentanglement from an initial product state.

The key technical step in both cases is a mapping of the quantum pseudothermalization problem onto the equilibration of certain classical Markov chains over subsets of the computational basis—with the size of subsets related to the number of state copies m available to the observer. This mapping allows us to make contact with a rich body of mathematical work on the equilibration of Markov chains on finite spaces, including the so-called *cutoff phenomenon* [37–41]. This phenomenon refers to the sudden equilibration that can be seen in random walks over highly-connected graphs (for example permutations of a deck of cards induced by a riffle shuffle [42]), in contrast with e.g. diffusion on a Euclidean lattice where equilibration is gradual and characterized by a dynamical scaling collapse $\sim t/L^z$, $z = 2$.

Based on this connection, we argue that pseudothermalization in our random circuit models happens in an asymptotically sharp fashion: our output states are easily distinguishable from Page states for a long time, until they abruptly (i.e., over a parametrically shorter window of time) become indistinguishable at the level of m copies, Fig. 1(c). This dynamical transition in the distinguishability of low-entanglement states from Page states is a new fundamental phenomenon in the dynamics of isolated quantum many-body systems, that enriches and complements our growing understanding of thermal equilibrium at the level of higher statistical moments [19, 43–47] and opens a number of exciting directions for future work.

The rest of the paper is organized as follows. In Sec. II we provide a brief, self-contained review of some useful background: pseudoentanglement (Sec. II A), Markov chains on finite sets and the cutoff phenomenon (Sec. II B), and certain random walks over permutation groups (Sec. II C). We then introduce the general framework of pseudothermalization via automaton circuit dynamics in Sec. III, and apply it to the problem of spreading and generation of pseudoentanglement in Sec. IV and V respectively. Finally we summarize our results and list outstanding questions and future directions in Sec. VI.

II. REVIEW OF KEY CONCEPTS

Asymptotic notation

In this work we make extensive use of the following asymptotic notation. Given two functions $f, g : \mathbb{N} \mapsto \mathbb{R}$, we write:

- $f = o(g)$ if $\lim_{N \rightarrow \infty} f(N)/g(N) = 0$;
- $f = O(g)$ if $f(N) < Cg(N)$ for all N for some constant $C > 0$;

- $f = \Theta(g)$ if $f = O(g)$ and $g = O(f)$;
- $f = \Omega(g)$ if $g = O(f)$;
- $f = \omega(g)$ if $\lim_{N \rightarrow \infty} f(N)/g(N) = \infty$.

With a slight abuse of notation, we also write asymptotic upper and lower bounds as e.g. $\Omega(f) \leq g \leq O(h)$ to denote that $g = O(h)$ and $g = \Omega(f)$. We also use a tilde to denote when one of these conditions applies up to a polylog(N) factor: e.g. we may write $f \leq O(g(N)/\log(N))$ as $f \leq \tilde{O}(g)$.

A. Pseudoentanglement

An ensemble of quantum states on N qubits is said to be *pseudoentangled* if it cannot be distinguished from the unitarily invariant (Haar) random ensemble by looking at any poly(N) number of copies [28]. More precisely, defining the m -th moment operator

$$\rho_{\mathcal{E}}^{(m)} = \mathbb{E}_{\psi \sim \mathcal{E}}[|\psi\rangle\langle\psi|^{\otimes m}], \quad (1)$$

an ensemble \mathcal{E} is pseudoentangled¹ if

$$\left\| \rho_{\mathcal{E}}^{(m)} - \rho_{\text{Haar}}^{(m)} \right\|_{\text{tr}} = o(1/\text{poly}(N)) \quad (2)$$

whenever $m = O(\text{poly}(N))$. The trace norm $\|A\|_{\text{tr}} = \text{Tr}(\sqrt{A^\dagger A})$ characterizes the distinguishability between two quantum states: if $\|\rho - \sigma\|_{\text{tr}} = \epsilon$, then there is an observable² \mathcal{O} , with $-I \leq \mathcal{O} \leq I$, that gives $\text{Tr}(\mathcal{O}\rho) - \text{Tr}(\mathcal{O}\sigma) = \epsilon$; then an observer can tell apart ρ from σ by measuring \mathcal{O} a number of times $\sim 1/\epsilon^2$. This is the optimal way to distinguish two states [48]. Thus the meaning of Eq. (2) is that, when making joint measurements on m copies of states drawn from \mathcal{E} , an observer would need a *superpolynomial* number of experiments to tell the two ensembles apart. Since we require Eq. (2) to apply for all $m \leq O(\text{poly}(N))$, the states from \mathcal{E} necessarily appear to be Haar-random (and thus near-maximally entangled) to any observer with polynomial resources, even though they may in fact be much less entangled.

A simple pseudoentangled ensemble is given by random *subset phase states* [28]

$$|\psi_{S,f}\rangle = \frac{1}{|S|^{1/2}} \sum_{\mathbf{z} \in S} (-1)^{f(\mathbf{z})} |\mathbf{z}\rangle, \quad (3)$$

where f is a random Boolean function on $\{0, 1\}^N$ chosen uniformly at random, and S is a subset of bitstrings, $S \subset$

¹ The definition in Ref. [28] additionally requires the ability to prepare the ensemble efficiently through suitable pseudorandom primitives. We will not focus on that aspect in this work.

² One can write the observable as $\mathcal{O} = \Pi_+ - \Pi_-$, where Π_{\pm} are the projectors on positive (negative) eigenvalue subspaces of $\rho - \sigma$.

$\{0, 1\}^N$, chosen uniformly at random out of all subsets of some fixed cardinality $|S| = K$. We call this space of subsets Σ_K . Here K must scale suitably with the system size N : $\omega(\text{poly}(N)) \leq K \leq o(2^N)$. The role of K is to determine the actual entanglement of the states in the ensemble: we have the average von Neumann entropy

$$S_{\text{vN}}(A) \sim \min\{|A| \log 2, \log K\} \quad (4)$$

for all subsystems A (regardless of locality), due to the fact that K upper bounds the Schmidt rank of $|\psi_{S,f}\rangle$ on any bipartition of the N qubits. Thus the restriction on $K \geq \omega(\text{poly}(N))$ ensures that, e.g., the half-cut entanglement entropy can scale faster than $\log N$ (necessary so that the states cannot be efficiently distinguished from Haar-random ones by measuring their purity), and the restriction $K \leq o(2^N)$ ensures that it scales more slowly than the Page value $\simeq N \log(2)/2$ [21] (see Fig. 1(a,b)).

Very recently, Ref. [29] showed that the random phase factors are not necessary to have a pseudoentangled ensemble. Random *subset states* suffice:

$$|\psi_S\rangle = \frac{1}{|S|^{1/2}} \sum_{\mathbf{z} \in S} |\mathbf{z}\rangle, \quad (5)$$

with S drawn uniformly at random from Σ_K (subsets of the computational basis of cardinality K). This ensemble obeys

$$\|\rho_{\mathcal{E}}^{(m)} - \rho_{\text{Haar}}^{(m)}\|_{\text{tr}} \leq O\left(\frac{m^2}{K}\right) + O\left(\frac{mK}{D}\right), \quad (6)$$

with $D = 2^N$ the Hilbert space dimension. This is super-polynomially small if $\omega(\text{poly}(N)) \leq K \leq o(2^N/\text{poly}(N))$ and $m = O(\text{poly}(N))$.

B. Equilibration of Markov chains and cut-off phenomenon

A key technical step in this work will be to map the evolution of quantum distinguishability measures such as Eq. (2) to the equilibration of classical Markov chains over finite sets. For this purpose it is useful to briefly review some notations and facts about this topic, including the cut-off phenomenon which will play an important role in our results.

A Markov chain on a finite set can be simply defined by a stochastic matrix Γ_{ij} , with i, j ranging over the set. ‘Stochastic’ means that $\Gamma_{ij} \geq 0$, with $\sum_i \Gamma_{ij} = 1$ for all j . Γ_{ij} represents the probability of a transition from j to i . A state of the Markov chain is given by a probability distribution $p(i)$. In each time step, p is updated according to $p(i) \mapsto \sum_j \Gamma_{ij} p(j)$. We say that the Markov chain equilibrates if $\Gamma^t p$ converges to some late-time limit π as $t \rightarrow \infty$.

The equilibration of finite-sized Markov chains is characterized by two fundamental time scales [49]. The first is the *mixing time*,

$$t_{\text{mix}}(\epsilon) = \min\{t : \|p_t - \pi\|_{\text{tv}} \leq \epsilon\}, \quad (7)$$

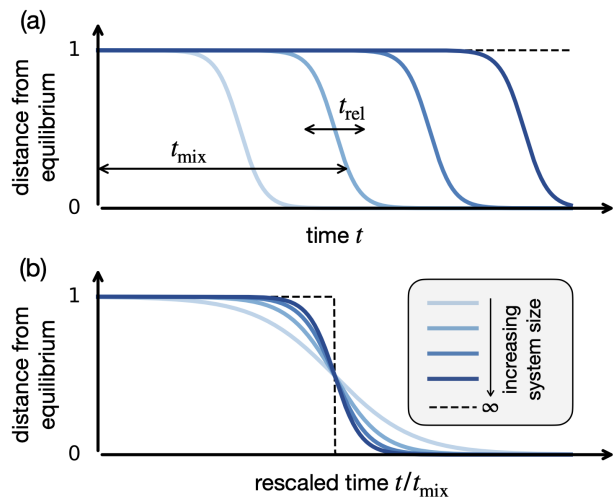


FIG. 2. Schematic of the cutoff phenomenon for Markov chains on finite sets. (a) A family of Markov chains on systems of size N has a cutoff if it exhibits “sudden” equilibration as $N \rightarrow \infty$, in the following sense: the total variation distance from equilibrium remains close to maximal for a time scale t_{mix} (*mixing time*), then decays to zero exponentially with a time constant t_{rel} (*relaxation time*) with $\lim_{N \rightarrow \infty} t_{\text{rel}}/t_{\text{mix}} = 0$. (b) Even though the relaxation time itself may be growing with N , upon rescaling time by $t \mapsto t/t_{\text{mix}}$ the approach to equilibrium becomes step-like as $N \rightarrow \infty$. In this sense there is a dynamically sharp equilibration transition.

describing the approach to the steady distribution. Here $\|\cdots\|_{\text{tv}}$ is the total variation norm, $\|p\|_{\text{tv}} = \frac{1}{2} \sum_i |p(i)|$, and one should maximize over all possible initial states. The second important time scale is the *relaxation time*, defined as the inverse spectral gap of the transition matrix Γ_{ij} :

$$t_{\text{rel}} = \frac{1}{1 - \lambda_1}, \quad (8)$$

where the spectrum of Γ_{ij} is given by $1 = \lambda_0 > \lambda_1 \geq \lambda_2 \geq \cdots > -1$. The relaxation time describes the asymptotic late-time decay towards the steady state.

In many cases of interest in physics, these two time scales have the same behavior: e.g., for the simple random walk on a line of length L , both time scales are $\propto L^2$. This gives a scale-invariant behavior, with the approach to equilibrium depending on the single ratio t/L^2 . However, in highly-connected spaces (e.g. expander graphs [50]) the two time scales can be different, with $t_{\text{rel}}/t_{\text{mix}} \rightarrow 0$ in the large-system limit. Such a separation of time scales, sketched in Fig. 2, is conjectured [39, 51] to give rise to the *cut-off phenomenon* [37–41]: an abrupt transition to equilibrium, defined by

$$\lim_{N \rightarrow \infty} \|p_{t(N)} - \pi\|_{\text{tv}} = \chi(\theta), \quad t(N) = t_{\text{mix}}(N) + \theta t_{\text{rel}}(N). \quad (9)$$

Here $\chi(\theta)$ is an N -independent function that goes to 1 as $\theta \rightarrow -\infty$ and to 0 as $\theta \rightarrow +\infty$. Informally, the to-

tal variation distance from equilibrium exhibits a scaling collapse as $N \rightarrow \infty$ on the form $\chi[(t - t_{\text{mix}})/t_{\text{rel}}]$, where the crucial observation is that the mid-point of the collapse (t_{mix}) and its width (t_{rel}) scale differently in the large-system limit: $t_{\text{rel}} = o(t_{\text{mix}})$. In other words, if we express time in units of t_{mix} , the distance from equilibrium becomes *step-like* in the infinite-system limit, going from almost-maximal to almost-zero over a vanishingly narrow window of time, $1 \pm t_{\text{rel}}/t_{\text{mix}}$. This is sketched in Fig. 2(b).

C. Random walks on permutation groups

In this work we will be especially interested in Markov chains over permutation groups and related processes. Here we give a brief review of some essential concepts [49].

Consider a graph (V, E) with vertices $V = \{v_i\}$ and edges $E = \{(v_i, v_j)\}$. The *interchange process* (IP) is a Markov chain over the permutation group $\mathcal{S}_{|V|}$ whose unit step consists of drawing an edge $(v_i, v_j) \in E$ uniformly at random and transposing its vertices v_i, v_j . The composition of t such transpositions $\tau_{i,j}$ produces a random element $\sigma_t = \tau_{i_t, j_t} \circ \dots \circ \tau_{i_1, j_1}$ of the permutation group $\mathcal{S}_{|V|}$. The IP is the Markov chain $\{\sigma_t\}_{t=0}^\infty$ on $\mathcal{S}_{|V|}$.

The IP induces other Markov chains of interest. The *random walk* (RW) with initial state v_i is the Markov chain $\{\sigma_t(v_i)\}_{t=0}^\infty$. This has the intuitive meaning we expect for a random walk on the graph (V, E) : a particle initialized at vertex v_i can hop with equal probability to any of its neighboring vertices. Additionally, the *exclusion process* with m particles (EX(m)) is defined as the Markov chain $\{\sigma_t(A)\}_{t=0}^\infty$ where $A \subset V$ is a collection of m distinct vertices, and $\sigma_t(A) \equiv \{\sigma_t(v_i) : v_i \in A\}$ is its image under permutation σ_t . This process describes the evolution of m indistinguishable, hard-core particles on the graph, where at each time step the occupation number of two neighboring vertices get swapped. When $m = 1$, this clearly reduces to the random walk: $\text{EX}(m) = \text{RW}$.

These three Markov chains are connected by a remarkable result known as *Aldous' spectral gap conjecture*³, which states that

$$t_{\text{rel}}^{\text{IP}} = t_{\text{rel}}^{\text{RW}} = t_{\text{rel}}^{\text{EX}(m)} \quad \forall m. \quad (10)$$

The inequality $t_{\text{rel}}^{\text{IP}} \geq t_{\text{rel}}^{\text{EX}(m)} \geq t_{\text{rel}}^{\text{RW}}$ is a simple consequence of the fact that RW and EX(m) are *sub-processes* of IP [52] (informally, they are projections of IP onto a smaller state space), and thus it holds also for other Markov chains on $\mathcal{S}_{|V|}$ beyond IP. However, the other direction of the inequality is highly nontrivial and is specific to IP, where it was conjectured in 1992 and proved in 2009 [52].

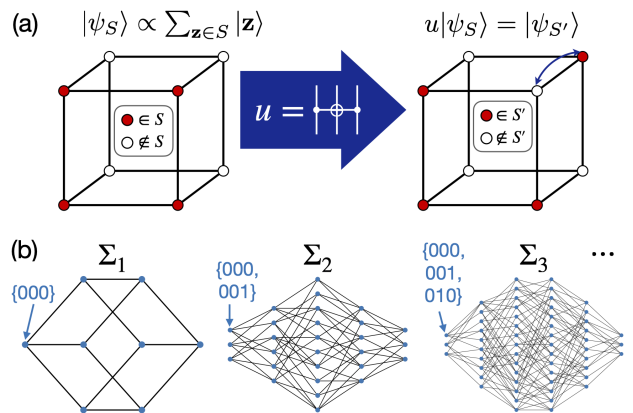


FIG. 3. (a) Subset states and their transformation under automaton gates, illustrated here for $N = 3$ qubits and a CCX gate. (b) Spaces of subsets of the computational basis, $\Sigma_m = \{S \subset \mathbb{Z}_2^N : |S| = m\}$, shown for $N = 3$ and $m = 1, 2, 3$. Vertices represent subsets $S \in \Sigma_m$, edges represent the action of an automaton gate set \mathcal{G} (self-edges are omitted for simplicity).

Beyond IP, in this work we will consider other Markov chains over permutation groups. In particular, we will consider a setting where the unit time step does not just transpose two neighboring vertices, like IP, but rather performs one of a more general set of “elementary permutations” in $\mathcal{S}_{|V|}$ sampled randomly at each time step. Such a process also gives a Markov chain over $\mathcal{S}_{|V|}$ and also induces “generalized exclusion processes” through the action of $\mathcal{S}_{|V|}$ on the subset spaces Σ_m , in the same way as IP induces EX(m). These “generalized exclusion processes” differ from the standard one as they can allow multiple particles to hop in a correlated way in each time step. Aldous’ spectral gap conjecture, Eq. (10), does not apply to this more general case. In Sec. IV C we will in fact encounter a case where the m -particle “generalized exclusion process” relaxes more slowly than the single-particle walk.

III. PSEUDOTHERMALIZATION IN AUTOMATON CIRCUITS

We aim to introduce models of quantum dynamics that achieve pseudoentanglement as their equilibrium state. However, fully-generic quantum dynamics tends to maximize actual entanglement. The easiest way to avoid this fate is to constrain the dynamics to preserve the ‘subset(-phase) state’ property, Sec. II A. Reversible classical circuits, also known as *automaton* circuits in the quantum context⁴ [33–36], have this property: an automaton circuit U_t corresponds to a permutation $\sigma_t \in \mathcal{S}_D$ of the

³ Despite the name, this is a proven theorem[52].

⁴ Note that some works use a different definition of automaton gates, which includes phases [35].

computational basis, $U_t|\mathbf{z}\rangle \equiv |\sigma_t\mathbf{z}\rangle$; thus, its action on a subset-phase state $|\psi_{S_0, f_0}\rangle$ is

$$U_t|\psi_{S_0, f_0}\rangle = \frac{1}{\sqrt{K}} \sum_{\mathbf{z} \in S_0} (-1)^{f_0(\mathbf{z})} |\sigma_t(\mathbf{z})\rangle = |\psi_{S_t, f_t}\rangle, \quad (11)$$

where $S_t = \{\sigma_t(\mathbf{z}) : \mathbf{z} \in S_0\} \equiv \sigma_t(S_0)$ is another subset of cardinality K , and $f_t \equiv f_0 \circ \sigma_t^{-1}$ is another phase function. In particular, if f_0 is uniformly random then so is f_t , and if f_0 is constant then so is f_t . It follows that automaton dynamics preserves the ‘subset(-phase) state’ property. Further, it preserves the cardinality of the subsets, K . The action of automaton gates on subsets is sketched in Fig. 3(a). An immediate consequence of Eq. (11) is that, under arbitrary automaton dynamics, the entanglement entropy about any cut cannot grow beyond $\log K$ (as K upper-bounds the Schmidt rank of the state). The maximum amount of entanglement is thus controlled by the choice of initial state, and saturation to the Page curve can be avoided.

In this work we consider the following type of dynamics. A distribution of initial states $|\psi_{S_0, f_0}\rangle$ is specified (these may be subset states or subset-phase states depending on the allowed values of f_0); then, each step of the time evolution consists of sampling an automaton gate u_i uniformly at random from a fixed gate set \mathcal{G} (we will discuss requirements on \mathcal{G} in the following) and applying it to the state. After t time steps, this results in an ensemble of time-evolved states $\{U_t|\psi_{S_0, f_0}\rangle = |\psi_{S_t, f_t}\rangle\}$ defined by all possible initial states and choices of $U_t = u_{i_t} u_{i_{t-1}} \cdots u_{i_1} \in \mathcal{G}^{\otimes t}$. The relevant notion of equilibration for this state ensemble is whether, at late times, it becomes *uniformly distributed* on the appropriate (subset or subset-phase) state space. If that is the case, and subject to usual constraints on the subset size K (see Sec. II A), then our dynamics achieves pseudoentanglement at late times. We call this condition *pseudothermalization*: while the upper limit K on the Schmidt rank prevents full thermalization (defined, for a model without conservation laws such as this one, by the approach to a Page state), this failure of thermalization may be practically undetectable, in a sense that is rigorously formalized through the concept of pseudoentanglement.

A first question to address is whether such equilibrium is achieved at all for a given automaton gate set \mathcal{G} . Let us focus on the subsets and neglect the phases for now. The action of the quantum circuits $U_t|\psi_{S_0}\rangle = |\psi_{S_t}\rangle$ defines a Markov chain $\{S_t\}$ over the space of size- K subsets of the computational basis,

$$\Sigma_K \equiv \{S \subset \{0, 1\}^N : |S| = K\}. \quad (12)$$

The transition matrix of the Markov chain, $\Gamma_{S', S}$, is specified by the gate set \mathcal{G} :

$$\Gamma_{S, S'} = \frac{1}{|\mathcal{G}|} \sum_{u \in \mathcal{G}} \delta_{S, u(S')}. \quad (13)$$

Viewing Γ as an adjacency matrix, we can thus picture the Σ_K spaces as graphs; some minimal examples are

shown in Fig. 3(b). To achieve pseudothermalization, the Markov chain $\{S_t\}$ must converge at late times to the uniform distribution on Σ_K , denoted here as π_K :

$$\lim_{t \rightarrow \infty} p_t = \pi_K, \quad (14)$$

where $p_t(S)$ is the probability distribution over subsets after t time steps. To guarantee the uniform distribution π_K as a unique steady state, the Markov chain must be [49]:

- (i) *Reversible*: the Markov chain transition matrix is symmetric, $\Gamma_{S', S} = \Gamma_{S, S'}$ for all S, S' . This property is ensured e.g. by picking a gate set \mathcal{G} such that $u^2 = I$ for all $u \in \mathcal{G}$.
- (ii) *Irreducible*: for any two states $S, S' \in \Sigma_K$, there exists a sequence of gates in \mathcal{G} that maps S to S' . Irreducibility will be discussed separately for each gate set \mathcal{G} in the following.
- (iii) *Aperiodic*: the chain can connect any two states S, S' with paths of any (sufficiently large) length⁵. One way to ensure aperiodicity is to make the chain ‘idle’, i.e. allow it to skip a step. This can be done by including the identity gate in \mathcal{G} .

For a gate set \mathcal{G} with all three properties above, we can conclude that $p_t \rightarrow \pi_K$ as $t \rightarrow \infty$. This suffices to establish pseudoentanglement at late times in two cases:

- when the initial state distribution is restricted to a constant phase function, e.g. $f_0 = 0$, we obtain the *random subset* ensemble [29];
- when the initial state distribution includes a uniformly random phase function f_0 , we obtain the *random subset-phase* ensemble [28].

Both of these ensembles are pseudoentangled, subject to certain constraints on K , as we reviewed in Sec. II A.

Having established that the steady-state ensembles in these two cases are pseudoentangled, it remains to understand how the system approaches this condition over the course of its dynamics, and what are the time scales involved. As already mentioned, we will call this process *pseudothermalization*, in analogy with how conventional thermalization in quantum many-body systems can be defined from the saturation of entanglement of local subsystems. Two key technical results will allow us to make progress on these questions by connecting pseudothermalization with the equilibration of certain classical Markov chains.

⁵ The prototypical counterexample is given by walks on bipartite graphs, where all paths connecting S to S' have the same length modulo 2. In that case the populations of the two partitions can keep oscillating indefinitely.

Proposition 1 (subset-phase states). *Consider an ensemble of subset-phase states $\mathcal{E}_p = \{|\psi_{S,f}\rangle : S \sim p, f \sim \text{unif.}\}$, specified by a uniformly random distribution over phase functions and a general probability distribution p over Σ_K (subsets). We have, for all integers $1 \leq m \leq K$,*

$$\left\| \rho_{\mathcal{E}_p}^{(m)} - \rho_{\text{Haar}}^{(m)} \right\|_{\text{tr}} = 2 \|\Phi_{m \leftarrow K}[p] - \pi_m\|_{\text{tv}} + O\left(\frac{m^2}{K}\right) \quad (15)$$

Here $\|\cdots\|_{\text{tr}}$ and $\|\cdots\|_{\text{tv}}$ are the trace norm and total variation norm, respectively; $\rho^{(m)}$ denotes the m -th statistical moment of a state ensemble, i.e. $\rho_{\mathcal{E}_p}^{(m)} = \mathbb{E}_{S \sim p} \mathbb{E}_f [|\psi_{S,f}\rangle\langle\psi_{S,f}|^{\otimes m}]$ and $\rho_{\text{Haar}}^{(m)} = \int d\psi_{\text{Haar}} |\psi\rangle\langle\psi|^{\otimes m}$; and $\Phi_{m \leftarrow K}$ is a stochastic map from distributions on Σ_K to distributions on Σ_m , defined by

$$\Phi_{m \leftarrow K}[p](S') = \binom{K}{m}^{-1} \sum_{S \in \Sigma_K: S' \subset S} p(S). \quad (16)$$

Proof. See Appendix A. \square

If we take $m = \text{poly}(N)$ and $K = \omega(\text{poly}(N))$, then the error term on the RHS of Eq. (15) is negligible, and pseudoentanglement (defined by the LHS being small) is tied to the non-uniformity of the distribution $\Phi_{m \leftarrow K}[p]$ on Σ_m . If we view p as the distribution Σ_K induced by the action of a random automaton circuit, then $\Phi_{m \leftarrow K}[p]$ is the distribution induced by the same process on Σ_m (up to an average over initial states). We show this in Appendix B, along with other useful properties of the stochastic maps Φ . Then Eq. (15) maps pseudoentanglement onto the mixing of a classical Markov chain on Σ_m .

Proposition 2 (subset states). *Consider an ensemble of subset states $\mathcal{E}'_p = \{|\psi_S\rangle : S \sim p\}$, specified by a general probability distribution p over Σ_K (subsets). We have, for all integers $1 \leq m \leq K/2$,*

$$\left\| \rho_{\mathcal{E}'_p}^{(m)} - \rho_{\text{Haar}}^{(m)} \right\|_{\text{tr}} = \left\| \mathcal{M}_p^{(m)} \right\|_{\text{tr}} + O\left(\frac{m}{\sqrt{K}}\right). \quad (17)$$

Here $\mathcal{M}_p^{(m)}$ is a $|\Sigma_m| \times |\Sigma_m|$ matrix defined by

$$(\mathcal{M}_p^{(m)})_{S', S''} = \binom{K}{m}^{-1} \binom{K}{m+\delta} f_p^{(m+\delta)}(S' \cup S''), \quad (18)$$

$$f_p^{(m+\delta)} = \Phi_{m+\delta \leftarrow K}[p] - \pi_{m+\delta}, \quad (19)$$

where we use subsets $S', S'' \in \Sigma_m$ to index the matrix elements, and define $\delta \equiv |S' \setminus S''|$.

Proof. See Appendix C. \square

We again relate pseudoentanglement (the LHS of Eq. (17) being small) to the non-uniformity of certain probability distributions over subsets; except unlike the previous case, Eq. (15), here we have contributions from a family of distributions $\{\Phi_{m+\delta \leftarrow K}[p]\}_{\delta=0}^m$, rather than from the single distribution $\Phi_{m \leftarrow K}[p]$. If we view p as

arising from a Markov chain on Σ_K induced by a random automaton circuit dynamics, then the emergence of pseudoentanglement is again related—albeit in a less straightforward way—to the mixing of the associated Markov chains $\Phi_{m+\delta \leftarrow K}[p]$ on $\Sigma_{m+\delta}$, for all $\delta = 0, 1, \dots, m$.

Having reduced the problem of pseudothermization to that of equilibration of certain Markov chains (namely random walks over the subset spaces $\{\Sigma_m\}$, Fig. 3(b)), we are now in a position to study the problem quantitatively by leveraging known results on these processes, including those reviewed in Sec. II B and II C. In the following sections we consider several automaton gate sets \mathcal{G} and initial state distributions, and analyze the associated classical Markov chains to characterize the process of pseudothermization.

IV. SPREADING OF PSEUDOENTANGLEMENT

A. Motivation and setup

In this section, we study the problem of how pseudoentanglement spreads in space, focusing on the setting of a smaller pseudoentangled system placed in contact with a larger, trivial system. This problem is reminiscent of analogous settings in the dynamics of entanglement: e.g., the growth of entanglement after quantum quenches where thermalization may happen due to the spreading of entangled quasiparticles in space [53, 54], or the equilibration of quantum spin chains connected to thermal baths at their edges [55–58].

We consider a situation in which we are given a random subset-phase ensemble $\mathcal{E}_0 = \{|\psi_{S_0, f_0}\rangle : S_0 \sim \text{unif.}, f_0 \sim \text{unif.}\}$ on a system A of N_A qubits. We take $|S_0| = K$ with $\omega(\text{poly}(N_A)) < K < o(2^{N_A})$, so that the initial ensemble on A is pseudoentangled. We then introduce a system \bar{A} of $N - N_A$ ancillas initialized in the product state $|0\rangle^{\otimes N - N_A}$, and form a larger system $A\bar{A}$ of N qubits. This overall system is still in a subset-phase state, though not a uniformly-random one; the initial state indeed is of the form $|\psi_{S_0, f_0}\rangle \otimes |0\rangle^{\otimes N - N_A}$. We can straightforwardly redefine S_0 as a subset of the computational basis of the extended system $\{0, 1\}^N$ (rather than the original system $\{0, 1\}^{N_A}$), by padding each bitstring with $N - N_A$ trailing zeros: $\mathbf{z} = (z_1, \dots, z_{N_A}) \mapsto (z_1, \dots, z_{N_A}, 0, \dots, 0)$. The phase function f_0 is never evaluated on any bitstrings outside the original ones, so it can be trivially extended to a uniformly random binary function on $\{0, 1\}^N$. Thus after including the ancillas, we have a subset-phase ensemble with uniformly random phases, but highly-correlated subsets. These states are manifestly not pseudoentangled—one can efficiently distinguish them from Haar-random states by, e.g., measuring $\langle Z_j \rangle$ for any $j > N_A$.

We then place the original system and ancillas into contact by allowing them to evolve together under automaton circuit dynamics, as discussed in Sec. III. The

question we aim to address is if and how pseudoentanglement is achieved on the entire system of N qubits over the course of the evolution. As the phases are already randomized, it is sufficient to focus on the subsets.

A first apparent constraint is that the value of K is conserved, even as we add the ancillas: even assuming that the subsets indeed equilibrate to the uniform distribution, pseudoentanglement requires $\omega(\text{poly}(N)) < K < o(2^N)$ (see Sec. II A). Combining these constraints with the analogous ones from the initial state ($N \mapsto N_A$) yields the overall constraint⁶

$$\omega(\text{poly}(N)) < K < o(2^{N_A}). \quad (20)$$

In particular this implies that N_A must grow faster than $\log(N)$. Intuitively this means that the number of ancillas added to the original system cannot be too large, otherwise one would “dilute” the initial pseudoentanglement too much.

Assuming Eq. (20), it remains to analyze the equilibration of subsets toward the uniform distribution under the chosen model of automaton dynamics. In the rest of this section, we discuss how to achieve this under two automaton gate sets \mathcal{G} , one made of all-to-all gates and the other of local gates.

B. All-to-all circuit model

We start by analyzing a model with a high degree of mathematical tractability, that comes at the cost of all-to-all interactions and exponentially-long equilibration time scales. We emphasize that these latter aspects are not at all necessary to pseudothermization in general, and are in fact absent from another model that we study next, in Sec. IV C.

We consider a gate set made of *globally-controlled* NOT gates: $\mathcal{G} = \{C_{\mathbf{a}}^{(N-1)} X_i\}$, where $C_{\mathbf{a}}^{(N-1)} X_i$ flips qubit i if and only if the remaining $N - 1$ qubits are in computational basis state $|\mathbf{a}\rangle$. There are $ND/2$ gates in \mathcal{G} : N choices for the target i and $2^{N-1} = D/2$ choices for the control string \mathbf{a} . The resulting circuit is illustrated in Fig. 4(a).

Viewed as a permutation of the hypercube \mathbb{Z}_2^N , the gate $C_{\mathbf{a}}^{(N-1)} X_i$ is simply a transposition of two neighboring vertices,

$$(\mathbf{a}_{1:i-1}, 0, \mathbf{a}_{i+1:N}) \xleftrightarrow{C_{\mathbf{a}}^{(N-1)} X_i} (\mathbf{a}_{1:i-1}, 1, \mathbf{a}_{i+1:N}) \quad (21)$$

(we use the shorthand $\mathbf{a}_{i:j} = (a_i, \dots, a_j)$). Clearly by a sequence of such neighbor transpositions one can trans-

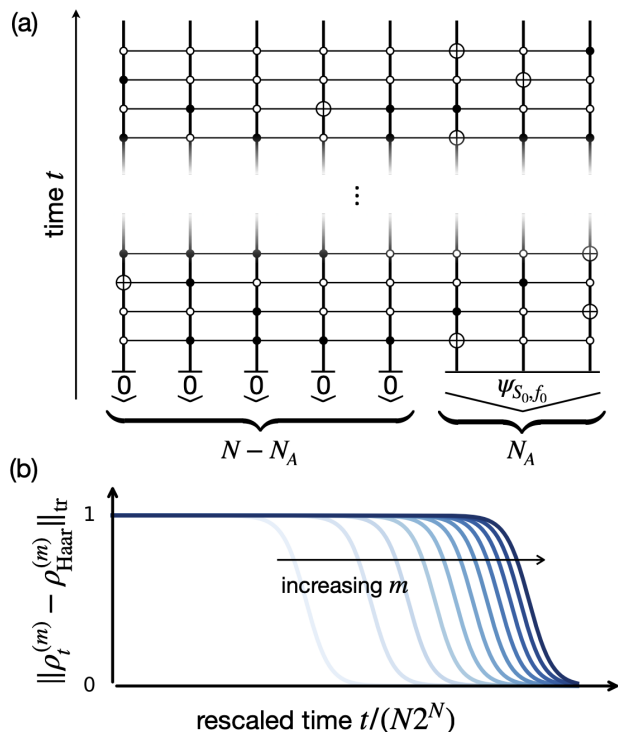


FIG. 4. All-to-all automaton circuit model for pseudoentanglement spreading. (a) Sketch of the circuit, showing a subset-phase initial state $|\psi_{S_0, f_0}\rangle$ on subsystem A along with $|0\rangle^{\otimes N-N_A}$ on the rest of the system, and a sequence of random globally-controlled NOT gates, $C_{\mathbf{a}}^{(N-1)} X_i$. Note that the controls come in two variations, open and solid circles, representing control on 0 and 1 respectively. (b) Sketch of the exact result Eq. (25) for the pseudothermization transitions in this model. Consecutive pseudothermization times $t_{\text{PTherm}}^{(m)}$, $t_{\text{PTherm}}^{(m+1)}$ are not sharply separated.

pose two arbitrary vertices⁷ $\mathbf{x} \leftrightarrow \mathbf{y}$; with these one can generate the whole permutation group \mathcal{S}_D . It follows that \mathcal{G} induces an irreducible Markov chain on Σ_m for all values of m . The Markov chains induced by \mathcal{G} on the subset spaces $\{\Sigma_m\}$ are also clearly reversible ($C_{\mathbf{a}}^{(N-1)} X_i$ is its own inverse) and aperiodic (it is always possible to draw a value of \mathbf{a}, i such that $C_{\mathbf{a}}^{(N-1)} X_i$ acts trivially on all bitstrings in S , making the walk idle). By the discussion in Sec. III we have that the unique steady state of the Markov chain on Σ_K is the uniform distribution π_K . Thus at late times this dynamics produces the random subset-phase state ensemble over the entire system, which in the relevant regime of (K, N) is pseudoentangled.

Having addressed the $t \rightarrow \infty$ limit of the dynamics, it remains to understand how pseudoentanglement

⁶ Some examples of parameters satisfying these constraints are as follows: $N_A = N/2$, $K = \exp(N^{1/2})$; $N_A = N^{1/2}$, $K = \exp(N^{1/4})$; $N_A = (\log N)^2$, $K = N^{\log \log N}$. These examples are purely illustrative; in the following we will not assume anything about N , N_A , K other than Eq. (20).

⁷ Given a path from \mathbf{x} to \mathbf{y} on the hypercube, the sequence of neighbor transpositions along the path and back has the effect of transposing \mathbf{x} and \mathbf{y} while leaving all other sites fixed.

is achieved as a function of time. To this end, we can use Proposition 1, which relates the m -copy distinguishability between the time-evolved state ensemble \mathcal{E}_t and the Haar ensemble to the mixing of a Markov chain $\Phi_{m \leftarrow K}[p_t]$ on Σ_m .

We note that the Markov chain on the permutation group \mathcal{S}_D induced by this gate set \mathcal{G} is precisely the interchange process (IP) on the hypercube \mathbb{Z}_2^N , reviewed in Sec. II C: each gate picks an edge of the hypercube uniformly at random and transposes its two vertices. It follows that the Markov chains $\Phi_{m \leftarrow K}[p_t]$ over the spaces of subsets Σ_m are exactly the exclusion processes $\text{EX}(m)$. These are well-studied problems for which we can rely on powerful known results.

First of all, Aldous' spectral gap conjecture [52], Eq. (10), states that the relaxation time of $\text{EX}(m)$ is equal, for all m , to the relaxation time of the simple random walk (RW). The simple random walk on the hypercube can be solved straightforwardly (see Appendix D 1), and one finds⁸ $t_{\text{rel}}^{\text{RW}} = ND/4$; therefore

$$t_{\text{rel}}^{\text{EX}(m)} = t_{\text{rel}}^{\text{RW}} = \frac{ND}{4} \quad \forall m. \quad (22)$$

Secondly, the mixing time for $\text{EX}(m)$ was recently solved [59] and was found to scale as

$$t_{\text{mix}}^{\text{EX}(m)} \sim ND \log(Nm). \quad (23)$$

Due to Proposition 1, this mixing time is also the time taken to achieve m -copy pseudothermalization.

Based on Eq. (22) and (23), we see that

$$t_{\text{mix}}^{\text{EX}(m)} / t_{\text{rel}}^{\text{EX}(m)} \sim \log(Nm) \xrightarrow{N \rightarrow \infty} \infty. \quad (24)$$

This asymptotic separation between the scaling of relaxation and mixing times is a necessary condition for a *cut-off phenomenon*, reviewed in Sec. II B. It was conjectured that in sufficiently “generic” models, such separation should also be a sufficient condition⁹. This cutoff effect would imply a sequence of dynamical transitions in our dynamics: for any moment $m \leq \text{poly}(N)$, there is a time scale at which the ensemble of output states

becomes indistinguishable from Haar-random at the m -copy level; this m -copy *pseudothermalization time* in this model is given by

$$t_{\text{PTerm}}^{(m)} \sim N2^N [\log(mN) \pm O(1)], \quad (25)$$

with the \pm term denoting the temporal width of the dynamical crossover to equilibrium. This result is sketched in Fig. 4(b). We note that, while each pseudothermalization transition is sharp (in the sense of $t_{\text{rel}}^{(m)} / t_{\text{mix}}^{(m)} \rightarrow 0$ at large N), consecutive transitions $t_{\text{PTerm}}^{(m)}, t_{\text{PTerm}}^{(m+1)}$ are *not* sharply separated. This is due to the slow growth of $t_{\text{mix}}^{(m)}$ with m , namely the fact that $[t_{\text{mix}}^{(m+1)} - t_{\text{mix}}^{(m)}] / t_{\text{rel}}^{(m)} \sim \log \frac{m+1}{m}$ does not diverge (and in fact it goes to zero at large m).

This exactly solvable model serves as a nice illustration of the idea of pseudothermalization, including the possible emergence of a cutoff phenomenon. At the same time, it has several drawbacks: the all-to-all interactions require complex couplings or compilation into deep local circuits; even worse, the resulting time scales for relaxation and mixing are exponentially long in system size. However, these limitations are artifacts of the model, and not intrinsic to the concept of pseudoentanglement or pseudothermalization. Below we introduce a *local* automaton gate set that does not suffer from these issues.

C. Local circuit model

In the interest of building a more physically realistic model of dynamics, we seek to restrict the gate set \mathcal{G} to geometrically local gates on a d -dimensional array of qubits.

The simplest automaton gate set comprises just local bit flips: $\mathcal{G} = \{X_i\}_{i=1}^N$. It is straightforward to see that the action of \mathcal{G} on Σ_1 is irreducible (we can map any bitstring to any other via bitflips); however it is already not irreducible on Σ_2 : given a set $S = \{\mathbf{z}, \mathbf{z}'\}$, the “relative coordinate” $\mathbf{z} \oplus \mathbf{z}'$ is invariant under bit flips. Moving up in complexity, one might try two-qubit automaton gates, generated by NOTs and CNOTs; however, it is possible to show that these gates are also insufficient to achieve irreducibility on Σ_m above $m = 3$. Three-qubit automaton gates, on the other hand, can induce irreducible and aperiodic Markov chains on Σ_m for all $m \leq D/4$, as we show in Appendix E.

In particular, for the case of a one-dimensional qubit array, we consider the gate set $\mathcal{G} = \{u_{iab} = C_{i-1,a} C_{i+1,b} X_i\}$ where $a, b \in \{0, 1\}$ label a control bitstring and $i \in [N]$ labels the target site (we take periodic boundary conditions, identifying $i = 0$ and $i = N$), as shown in Fig. 5(a). The u_{iab} gate flips qubit i if and only if its left neighbor $i - 1$ is in state a and its right neighbor $i + 1$ is in state b . There are N choices for the target site i and 4 choices for the control string (a, b) , giving a total of $4N$ gates in \mathcal{G} . Up to bit flips, each u_{iab} is a Toffoli gate. It is easy to see that the gate set

⁸ The exponential scaling in N is due to the fact that each elementary transposition of hypercube vertices is exponentially unlikely to cause the random walker to hop: only N gates out of $ND/2$ cause a nontrivial hop. The conventional result for a random walker who hops once per unit time is $t_{\text{rel}}^{\text{RW}} = N/2$; rescaling this by the average number of gates between hops ($D/2$) yields Eq. (22) (see also more detailed derivation in Appendix D 1).

⁹ Note that the condition $t_{\text{rel}} = o(t_{\text{mix}})$ is not sufficient to get a cutoff phenomenon in total variation distance in general (on the other hand it *is* sufficient if the distance from equilibrium is measured with a L^p norm, $p > 1$ [39]). It is possible to have a so-called *pre-cutoff* where multiple step-like transitions arise in the total variation distance. However, this usually requires some particular structure in the connectivity of the underlying graph (e.g. bottlenecks separating highly connected regions).

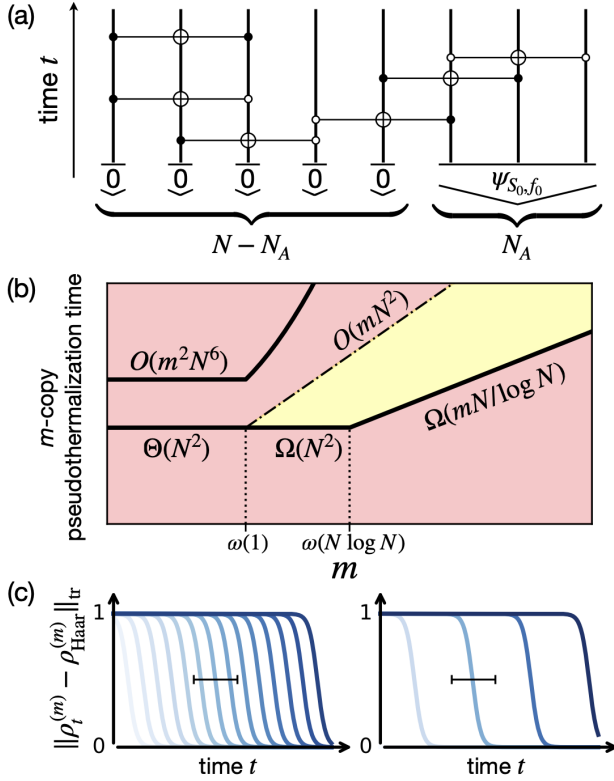


FIG. 5. Local automaton circuit model for the spreading of pseudoentanglement. (a) Circuit model, analogous to Fig. 4 but with local CCX gates. (b) Schematic summary of bounds on the pseudothermalization time. Solid lines denote unconditional bounds while the dot-dashed line depends on Conjecture 1. The yellow area indicates allowed scalings. The lower bounds come from Eq. (30) (counting) and Eq. (31) (locality). The dashed-line upper bound comes from Eq. (29); the solid-line upper bound is Eq. (27). (c) Consecutive m -copy pseudothermalization transitions in this model may be overlapping (left) or sharply separated (right) in the thermodynamic limit: answering this question requires tighter bounds on the mixing time.

generates CX gates, SWAP gates, and bit flip gates as well—it in fact generates arbitrary *even* permutations of the computational basis, see Appendix E.

1. First moment

We start our analysis of this dynamics from the first moment, $m = 1$. The Markov chain on $\Sigma_1 \equiv \mathbb{Z}_2^N$ corresponds once again to the simple random walk on the hypercube, see Appendix D 1. With each gate the walker, a bitstring \mathbf{z} , stays in place with probability $3/4$ (if the control string a, b of the randomly-sampled u_{iab} gate does not match \mathbf{z}), otherwise it hops to a neighbor (a bitstring \mathbf{z}' differing only at one bit) chosen uniformly at random based on the value of $i \in [N]$. Using again the known results for the simple random walk on the hypercube,

Appendix D 1, we have

$$t_{\text{rel}}^{(1)} = 2N, \quad t_{\text{mix}}^{(1)} \sim N \log(N), \quad (26)$$

with the only difference from the case of Sec. IV B (with $m = 1$) being the different idling time between hops (4 instead of $D/2$). Just like in Sec. IV B, the random walk exhibits a cutoff [60], with the approach to equilibrium taking place in a relatively narrow time window, $t \sim N[\log N \pm O(1)]$. Intuitively, to achieve equilibrium the walker has to hop in all N directions with high probability (equivalently, all N qubits need to be flipped with high probability). This is an instance of the so-called “coupon collector’s problem”, which gives a scaling $\sim N \log(N)$. Note that time t is defined as total number of gates acting on the system; defining a rescaled time $\tau \equiv t/N$ such that each qubit flips of order once per unit τ , equilibration happens at $\tau \sim \log(N) \pm O(1)$.

2. Higher moments: Relaxation time

For higher moments $m > 1$, unlike the all-to-all model of Sec. IV B, the Markov chain on Σ_m is not exactly solvable (to our knowledge). To make progress we resort to a combination of rigorous bounds and numerical calculations.

We begin by analyzing the relaxation time $t_{\text{rel}}^{(m)}$ of the Markov chain on Σ_m , for $m > 1$, through exact numerical diagonalization of the Markov chain transition matrix Γ for accessible values of the system size N and subset size m . Exact diagonalization is limited by the dimensionality of the problem, given by the size of the subset space¹⁰ $|\Sigma_m| = \binom{D}{m} = \binom{2^N}{m}$. This grows explosively with m and N , limiting us to $mN \lesssim 30$.

Results for the spectra of Γ for different system sizes N and moments m are shown in Fig. 6(a). Recall that the spectrum of Γ has a leading eigenvalue $\lambda_0 = 1$, associated to the uniform distribution π_m (its unique steady state), and then subleading eigenvalues $1 > \lambda_1 \geq \lambda_2 \geq \dots$; the inverse spectral gap defines the relaxation time: $t_{\text{rel}}^{(m)} = 1/(1 - \lambda_1)$. For $m = 1$ the problem reduces once again to the simple random walk on the hypercube \mathbb{Z}_2^N , so the leading eigenvalue $\lambda_0 = 1$ is followed by a N -fold degenerate multiplet of eigenvalues $\lambda_1 = 1 - \frac{1}{2N}$, giving the relaxation time $t_{\text{rel}}^{(1)} = 2N$. These eigenvalues appear in the spectra for all values of m , where they are associated to the N components of the dipole moment of the m -particle distribution on the hypercube, see Appendix D 2.

However, for $m \geq 2$, we observe a new second-largest eigenvalue in the spectrum of Γ , $1 - 1/2N < \lambda_1 < 1$, giving longer relaxation times $t_{\text{rel}}^{(m)} > t_{\text{rel}}^{(1)}$. This is unlike the all-to-all model of Sec. IV B, where Aldous’ spectral gap conjecture Eq. (10) (see Sec. II C) forces $t_{\text{rel}}^{(m)}$ to be

¹⁰ The effective dimensionality is lower due to the problem’s translation and reflection invariance, but only by a factor of $\approx N$.

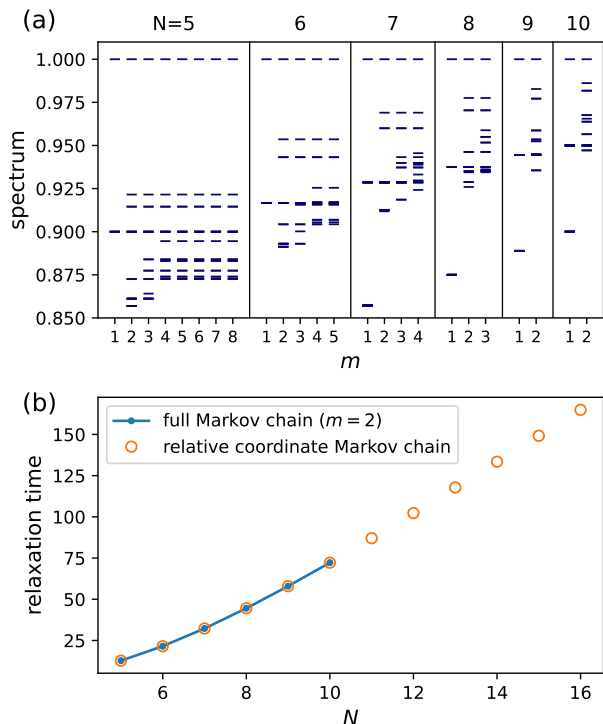


FIG. 6. (a) Largest 20 eigenvalues of the Markov chain transition matrix $\Gamma_{S,S'}$ for different system sizes $N = 5, \dots, 10$ (indicated at the top of each panel) and subset sizes m , obtained from exact diagonalization (Lanczos). We consider all pairs (N, m) such that the dimension $|\Sigma_m| = \binom{2^N}{m}$ of the transition matrix is below 2×10^7 . For $m = 1$ we recover the spectrum of the single-particle random walk, $1 - \frac{c}{2^N}$, $c \in [N]$; a new leading eigenvalue $\lambda_1 > 1 - \frac{1}{2^N}$ appears for $m = 2$ and persists for all accessible values of m . (b) Relaxation time $t_{\text{rel}} = 1/(1 - \lambda_1)$ as a function of system size N for two Markov chains: the full Markov chain over pairs of bitstrings, Γ (λ_1 taken from (a), $m = 2$), and the random walk of the “relative coordinate” $\Gamma|_R$ (see main text). The two agree to numerical precision up to the system sizes accessible to both ($N \leq 10$); the data suggests an asymptotically linear scaling of $t_{\text{rel}}^{(2)}$ with N .

m -independent. Nonetheless, Fig. 6(a) shows no further m -dependence in λ_1 beyond $m = 2$. This suggests that $m = 1$ is special in this problem.

By numerical inspection, we find that the new slowest mode of Γ for $m = 2$, the function $f_1(S)$ such that $\Gamma f_1 = \lambda_1 f_1$, depends on the subset $S = \{\mathbf{z}, \mathbf{z}'\}$ only through the “relative coordinate” $\mathbf{r} \equiv \mathbf{z} \oplus \mathbf{z}'$. In Appendix D3 we show that the subspace R spanned by functions that depend on S only through the relative coordinate \mathbf{r} is invariant under the Markov chain. Thus we can block-diagonalize $\Gamma = \Gamma|_R \oplus \Gamma|_{R^\perp}$, where $\Gamma|_R$ describes a random walk of \mathbf{r} . Numerical diagonalization confirms that the leading eigenvalue λ_1 of Γ indeed comes from the $\Gamma|_R$ block: results for λ_1 agree to numerical precision between the two Markov chains. Furthermore, due

to the reduced dimensionality ($\sim D$ for $\Gamma|_R$ compared to $\sim D^2$ for the full Γ), we are able to numerically diagonalize the restricted Markov chain up to larger values of system size N . Results, shown in Fig. 6(b), indicate a clear linear scaling $t_{\text{rel}}^{(2)} = \Theta(N)$.

These observations ($t_{\text{rel}}^{(2)}$ scaling linearly in N and $t_{\text{rel}}^{(m)}$ being independent of $m \geq 2$ for all numerically accessible values) lead us to formulate the following conjecture:

Conjecture 1 (scaling of relaxation time). *For all $m \geq 2$, the Markov chain on Σ_m induced by the local automaton gate set \mathcal{G} has relaxation time $t_{\text{rel}}^{(m)} = \Theta(N)$, independent of m .*

We cannot rule out the possibility of further changes in the relaxation times $t_{\text{rel}}^{(m)}$ at larger values of m beyond those accessible in numerics. In Appendix F we show an unconditional upper bound

$$t_{\text{rel}}^{(m)} \leq O(mN^5), \quad (27)$$

which we believe is very loose. Proving (or disproving) our Conjecture 1, and/or tightening bounds around the relaxation times $t_{\text{rel}}^{(m)}$, are left as goals for future research. However, since a precise determination of relaxation times in the arguably simpler models of Ref. [61–63] is still lacking, we suspect these may be hard problems.

3. Higher moments: Mixing time

Assuming the validity of Conjecture 1, $t_{\text{rel}}^{(m)} = \Theta(N)$, we move on to the question of mixing times. A general two-sided bound on the mixing time in terms of the relaxation time is given by [49, 64]

$$(t_{\text{rel}}^{(m)} - 1) \log\left(\frac{1}{2\epsilon}\right) \leq t_{\text{mix}}^{(m)}(\epsilon) \leq t_{\text{rel}}^{(m)} \log(|\Sigma_m|/\epsilon), \quad (28)$$

where ϵ is the accuracy threshold on total variation distance used to define mixing; see Sec. IIB. We take $\epsilon = 1/4$ in the following. Plugging Conjecture 1 in Eq. (28) yields the asymptotic bounds

$$\Omega(N) \leq t_{\text{mix}}^{(m)} \leq O(mN^2), \quad (29)$$

where we use $\log |\Sigma_m| = \log \binom{D}{m} \leq mN$.

The lower bound Eq. (28) clearly cannot be used to gap $t_{\text{mix}}^{(m)}$ away from $t_{\text{rel}}^{(m)}$, which is the necessary condition for a cut-off phenomenon. To study the possible presence of a cut-off we must find stronger lower bounds on the mixing time. We show two such bounds next.

Fact IV.1 (counting bound). *For all m , the mixing for the Markov chain induced by the local gate set \mathcal{G} obeys*

$$t_{\text{mix}}^{(m)} \geq \Omega(mN/\log N). \quad (30)$$

Proof. Let us count the number of states that can be reached from an initial state $S_0 \in \Sigma_m$ in t time steps.

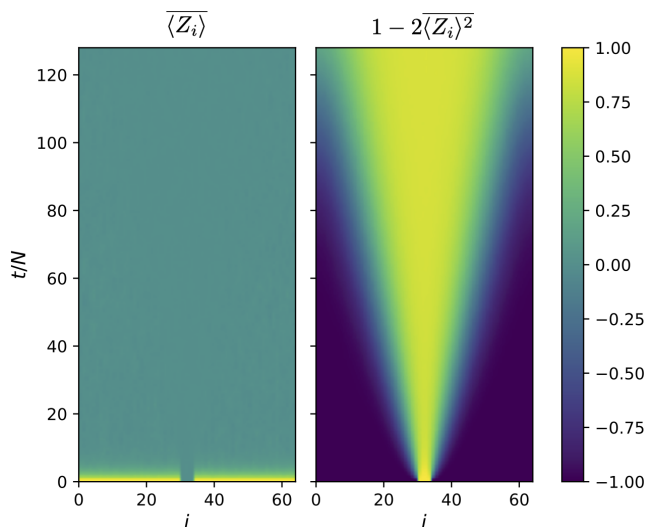


FIG. 7. Numerical simulation of local random automaton circuits on a chain of $N = 64$ qubits, initialized in the product state $|0\rangle^{\otimes N-N_A} \otimes |+\rangle^{\otimes N_A}$ with $N_A = 4$ (we shift the $|+\rangle$ qubits to the center of the plot for clarity). Data averaged over 10^4 random circuit realizations. Left: local expectation values averaged over circuit realizations, $\overline{\langle Z_i \rangle}$, can relax under local bit flips and thus equilibrate quickly. Right: higher-moment quantities, such as $\overline{\langle Z_i \rangle^2}$ (related to the variance of $\langle Z_i \rangle$ across circuit realizations), require the propagation of coherence across the system. Their equilibration is thus constrained by a light cone, $t/N \geq \Omega(N)$. Note t is the total number of applied gates.

As each state is connected to at most $|\mathcal{G}| = 4N$ different states, the volume of a ball of radius t in Σ_m (viewed here as a graph with edges given by the action of \mathcal{G}) is at most $(4N)^t$. To achieve mixing, the distribution p_t needs to be supported on, say, at least $1/2$ of the states. Thus we must have $(4N)^t \geq |\Sigma_m|/2$, giving $t \log(4N) \geq \log \binom{D}{m} \geq mN$. \square

Fact IV.2 (locality bound). *For all $m \geq 2$, the mixing for the Markov chain induced by the local gate set \mathcal{G} on a 1D qubit chain obeys*

$$t_{\text{mix}}^{(m)} \geq \Omega(N^2). \quad (31)$$

Proof. It is easy to see that, starting from a subset S_0 where all bitstrings agree outside the subsystem A ($z_j = 0$ for all sites $j = 1, \dots, N - N_A$, for all bitstrings $\mathbf{z} \in S_0$), the region outside a “light cone” emanating from A remains in a product state: local automaton gates cannot create superpositions, so coherence must spread outward from A one gate at a time. As the gate sequence is random, the light cone fluctuates instance by instance, however its width is bounded above¹¹ by

¹¹ We can bound $\ell(t)$ above by noting that $\ell(t+1) = \ell(t) + 1$ with

$\ell(t) \leq N_A + 2vt/N$, for some constant ‘butterfly velocity’ v , with finite probability. Whenever $\ell(t) < N$, the distribution $p_t(S)$ is supported only on a small fraction of the state space Σ_m (all subsets S that correspond to a product state outside the light cone), and thus must be far from uniform¹². Equilibrium can only be reached after the light cone has spread across the whole system, giving $\ell(t) \geq \Omega(N)$ or $t \geq \Omega(N^2)$. \square

We note that, while the counting bound (Eq 30) applies to all m , the locality bound (Eq. 31) does not apply to $m = 1$ (indeed we have $t_{\text{mix}}^{(1)} \sim N \log N$, Eq. (26)). This is because “subsets” with $m = 1$ are just individual bitstrings, so equilibration does not require coherence (i.e. superpositions) to spread across the system. This physical difference in the effects of locality is illustrated in Fig. 7. We show results of numerical simulations for circuit-averaged quantities $\overline{\langle Z_i \rangle}$ (a first-moment quantity that can equilibrate under local bitflips) in Fig. 7(a) and $\overline{\langle Z_i \rangle^2}$ (a second-moment quantity that requires superpositions to equilibrate) in Fig. 7(b). Again we recall that “time” t here is measured as total number of gates in the circuit, so $t \sim N^2$ here denotes ballistic, not diffusive, spreading of correlations.

Putting Facts IV.1 and IV.2 together with the upper bound Eq. (29), we arrive at

$$\Omega(N^2, mN/\log(N)) \leq t_{\text{mix}}^{(m)} \leq O(mN^2). \quad (32)$$

These bounds are summarized in Fig. 5(b). We remark again that the upper bound Eq. (29) assumes Conjecture 1; an unconditional, likely loose bound $t_{\text{mix}}^{(m)} \leq O(m^2 N^6)$ can be derived based on Eq. (27) (see Appendix F).

Several interesting consequences follow from Eq. (32). First of all, independently of m , we have

$$\lim_{N \rightarrow \infty} t_{\text{mix}}^{(m)}/t_{\text{rel}}^{(m)} = \infty, \quad (33)$$

which is a necessary condition for a cut-off, see Sec. II B. We thus conjecture the presence of asymptotically sharp pseudothermalization transitions in this model. While numerical simulations are strongly limited by the explosive growth of the state space $|\Sigma_m| = \binom{2^N}{m}$, results of exact simulations of $N = 5$ qubits, shown in Fig. 8, are consistent with the emergence of a cutoff—we clearly see the development of a plateau, followed by a decay $\sim \lambda_1^{t-\delta t}$ of the total variation distance, with a temporal offset $\delta t \sim m$ in the accessible range¹³ $1 \leq m \leq 8$.

probability at most $2/N$ (the CCX gate must have the target qubit i at either light cone front), and $\ell(t+1) \leq \ell(t)$ otherwise. Then $\bar{\delta \ell} \leq 2/N$ and thus $\ell(t) \leq \ell(0) + 2t/N$ with finite probability. This gives an upper bound on the butterfly velocity $v \leq 1$.

¹² Another way to argue this is by the distinguishing statistics method in Ref. [49] applied to, e.g., $\overline{\langle Z_i \rangle^2}$ for a qubit i far from A .

¹³ $N = 5$, $m = 8$ yields $|\Sigma_8| = \binom{32}{8} \gtrsim 10^7$ states.

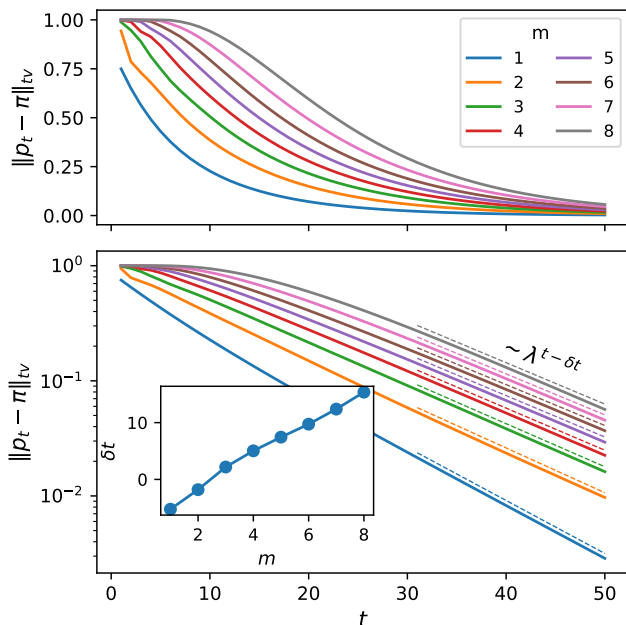


FIG. 8. Exact numerical simulation of the Markov chain induced by the local automaton gate set on $N = 5$ qubits for subset sizes $m = 1, \dots, 8$. The initial quantum state is taken to be $|00++\rangle$, a subset state with $K = 8$. The total variation distance from uniformity decays as $\|p_t - \pi\|_{\text{tv}} \sim \lambda^{t-\delta t}$ at late times (bottom panel, dashed lines). Fit results for λ (not shown) are consistent with the results of Fig. 6, with $\lambda \simeq 0.90$ for $m = 1$ and $\lambda \simeq 0.92$ for all $m \geq 2$; the temporal offset δt , a proxy for the mixing time (up to additive constants), is found to scale linearly in m (bottom panel, inset).

We can then break down the behavior of different moments m , based on their scaling with N , to obtain an interesting (though still incomplete) picture of the dynamics:

- (i) For constant m , we have $t_{\text{mix}}^{(m)} = \Theta(N^2)$, and thus the pseudothermization time

$$t_{\text{PTherm}}^{(m)} \sim N^2[1 \pm O(1/N)], \quad (34)$$

with the \pm term denoting the width of the time window in which the transition to equilibrium happens. This suggests a picture based on a ‘pseudothermization front’ spreading ballistically through the system, with fast equilibration behind the front, so that m -copy pseudothermization happens suddenly, and simultaneously for all constant m , once the front has swept across the system.

- (ii) In the intermediate range $\omega(1) \leq m \leq O(N \log N)$, our bounds are insufficient to pin down the scaling of $t_{\text{PTherm}}^{(m)}$; we have

$$t_{\text{PTherm}}^{(m)} \sim N^2[f(m) \pm O(1/N)], \quad (35)$$

for some function $\Omega(1) \leq f(m) \leq O(m)$. Depending on the scaling of $f(m)$, it is possible that the

‘pseudothermization front’ picture ceases to apply, with a parametrically slower equilibration behind the ballistic front and a separation of consecutive pseudothermization transitions $t_{\text{PTherm}}^{(m)}$, $t_{\text{PTherm}}^{(m+1)}$.

- (iii) At even higher moments $\omega(N \log N) \leq m \leq O(\text{poly}(N))$, the counting bound becomes dominant over the locality bound, so the ‘font’ picture is not relevant anymore. We have

$$t_{\text{PTherm}}^{(m)} \sim N[mg(N) \pm O(1)], \quad (36)$$

for some function $\Omega(1/\log N) \leq g(N) \leq O(N)$. Depending on the scaling of $g(N)$, consecutive pseudothermization times $t_{\text{PTherm}}^{(m)}$, $t_{\text{PTherm}}^{(m+1)}$ may be sharply separated, or the two crossover windows may overlap. These two options are sketched in Fig. 5(c).

- (iv) Finally, for $m \geq \omega(\text{poly}(N))$, we have $t_{\text{mix}}^{(m)} \sim m$ up to $\text{poly}(N)$ factors.

4. Higher dimension

The analysis above could be straightforwardly adapted to higher-dimensional qubit arrays. For example one can choose a gate set $\mathcal{G} = \{u_{i,\hat{v},\hat{w},a,b}\}$, with $i \in [N]$ a site, \hat{v}, \hat{w} two different directions on the lattice, and $a, b \in \{0, 1\}$ control bits, where the gate u flips qubit i iff its neighbors $i + \hat{v}$, $i + \hat{w}$ are in states a, b respectively. \mathcal{G} contains $4 \binom{2d}{2} N$ gates, with d the spatial dimension. In $d = 1$ one recovers the gate set used earlier (in that case the choice of directions $\hat{v} = +\hat{x}$, $\hat{w} = -\hat{x}$ is unique).

For constant d , all the results of this section proceed unchanged, except for the locality bound, Eq. (31); there, we must replace Eq. (31) with $t_{\text{mix}}^{(m)} \geq \Omega(N^{1+1/d})$, with d the spatial dimension. This still meets the requirement for a cut-off, Eq. (33), but is not enough to pin down the scaling of pseudothermization time at constant m : we have instead $\Omega(N^{1+1/d}) \leq t_{\text{mix}}^{(m)} \leq O(N^2)$.

Qualitatively, this opens the question of whether, in dimension $d \geq 2$, the ‘pseudothermization front’ picture still holds; i.e., if the state behind the light cone equilibrates quickly (which would give $t_{\text{mix}}^{(m)} \sim N^{1+1/d}$), or whether it equilibrates more slowly, in such a way that even after the light cone has swept through the whole system it is still possible to distinguish the states from Haar-random ones with a constant number of copies m .

V. GENERATION OF PSEUDOENTANGLEMENT

Thus far we have discussed the propagation of pseudoentanglement: we have taken initial states that already contain random subset-phase ensembles on subsystems, and studied how these turn into random subset-phase

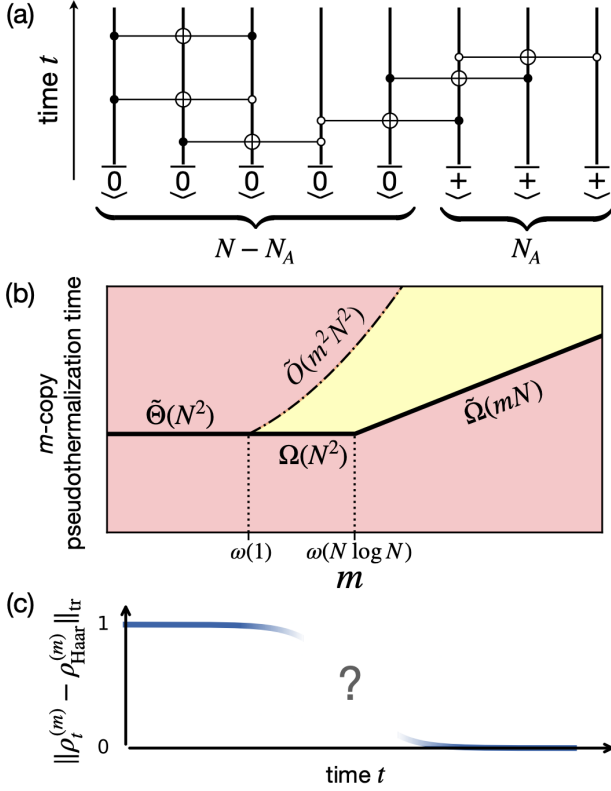


FIG. 9. Local automaton circuit model for the generation of pseudoentanglement from product states. (a) Circuit model: the same as Fig. 5(a) but with a product initial state $|0\rangle^{\otimes N-N_A} \otimes |+\rangle^{\otimes N_A}$ (no random phases). (b) Schematic summary of bounds for the pseudo-thermalization time. Solid lines indicate unconditional bounds while the dot-dashed line depends on Conjecture 1. Results are the same as in Fig. 5(b) but with a modified upper bound $\tilde{O}(m^2 N^2)$, Eq. (44). (c) Given the more complex mapping between quantum ensemble distinguishability and the mixing of classical Markov chains, Eq. (38-39), the precise nature of pseudo-thermalization (e.g., whether there is a cut-off) remains unclear in this case.

states on the whole system under automaton circuit dynamics. This approach was motivated partly by analogy with the problem of entanglement spreading in quantum quenches, and partly by technical simplifications that arise when random phases are already provided by the input states. In this section, we address the question of generating pseudoentanglement from initial product states. To avoid complications associated with random phases, we choose to focus on the *random subset states* introduced in Ref. [29] and reviewed in Sec. II A. We use only the local gate set of Sec. IV C.

Let us take an initial subset state

$$|\psi_{S_0}\rangle = |0\rangle^{\otimes N-k} \otimes |+\rangle^{\otimes k}, \quad (37)$$

corresponding to subset $S_0 = \{\mathbf{z} : z_1 = \dots = z_{N-k} = 0\}$ of cardinality $K = 2^k$, shown by Fig. 9(a). To be pseudoentangled, random subset ensembles need to have $\omega(\text{poly}(N)) \leq K \leq o(2^N/\text{poly}(N))$, therefore we take

the number of qubits initially in superposition, k , to be $\omega(\log N) \leq k < cN$ with $0 < c < 1$ a constant. After t time steps, we have a subset state $|\psi_{S_t}\rangle$ where S_t is a random variable on Σ_K distributed according to a time-evolved distribution p_t . To characterize the generation of pseudoentanglement, we look at the trace distance between m -th moment operators, $\|\rho_t^{(m)} - \rho_{\text{Haar}}^{(m)}\|_{\text{tr}}$, with $\rho_t^{(m)} = \sum_S p_t(S) |\psi_S\rangle \langle \psi_S|^{\otimes m}$. As long as $m \leq O(\text{poly}(N))$, the application of Proposition 2 yields

$$\|\rho_t^{(m)} - \rho_{\text{Haar}}^{(m)}\|_{\text{tr}} \simeq \|\mathcal{M}_{p_t}^{(m)}\|_{\text{tr}}, \quad (38)$$

$$(\mathcal{M}_{p_t}^{(m)})_{S', S''} = \binom{K}{m}^{-1} \binom{K}{m+\delta} f_{p_t}^{(m+\delta)}(S' \cup S''), \quad (39)$$

where $\delta \equiv |S' \setminus S''|$ is the difference between subsets $S', S'' \in \Sigma_m$ (so $S' \cup S'' \in \Sigma_{m+\delta}$), and

$$f_{p_t}^{(m+\delta)} = \Phi_{m+\delta \leftarrow K}[p_t] - \pi_{m+\delta} \quad (40)$$

is the deviation from uniformity of a Markov chain on $\Sigma_{m+\delta}$ induced by the random automaton circuit, as in Sec. IV.

In this case, the pseudo-thermalization problem is not directly mapped onto the mixing of a single classical random walk. Rather, it is mapped in a nontrivial way, via Eq. (39), to the mixing of $m+1$ distinct random walks, indexed by $\delta = 0, 1, \dots, m$, and distributed according to $\Phi_{m+\delta \leftarrow K}[p_t]$, defined by Eq. (16).

More specifically, the diagonal terms in $\mathcal{M}_{p_t}^{(m)}$ correspond to $\delta = 0$, i.e., to the walk on Σ_m distributed as $\Phi_{m \leftarrow K}[p_t]$. This is the same walk that controlled the spreading of pseudoentanglement in Sec. IV. However, the off-diagonal terms, corresponding to $\delta > 0$, make this problem more complex. While we do not have an exact solution in this case, one can still obtain nontrivial bounds on the pseudo-thermalization time $t_{\text{PTTherm}}^{(m)}$, as we discuss next.

First, a lower bound on $t_{\text{PTTherm}}^{(m)}$ is obtained by using the monotonicity of trace norm under quantum channels: $\|\mathcal{D}(\mathcal{M})\|_{\text{tr}} \leq \|\mathcal{M}\|_{\text{tr}}$, where \mathcal{D} is a dephasing super-operator that annihilates off-diagonal matrix elements: $[\mathcal{D}(\mathcal{M})]_{S', S''} = \delta_{S', S''} \mathcal{M}_{S', S'}$. This gives

$$\|\rho_t^{(m)} - \rho_{\text{Haar}}^{(m)}\|_{\text{tr}} \geq 2\|\Phi_{m \leftarrow K}[p_t] - \pi_m\|_{\text{tv}} \quad (41)$$

(up to negligible terms $O(m/\sqrt{K})$), which in turn implies

$$t_{\text{PTTherm}}^{(m)} \geq t_{\text{mix}}^{(m)}. \quad (42)$$

Here $t_{\text{mix}}^{(m)}$ is the mixing time of the Markov chain $\Phi_{m \leftarrow K}[p_t]$, studied in Sec. IV; the lower bounds we derived there thus apply directly to the pseudo-thermalization time in the present problem (in one spatial dimension):

$$t_{\text{PTTherm}}^{(m)} \geq \Omega(N^2, mN/\log(N)). \quad (43)$$

Furthermore, since the matrix $\mathcal{M}_{p_t}^{(m)}$ that controls pseudo-thermalization, Eq. (39), consists of differences $\Phi_{m+\delta\leftarrow K}[p_t] - \pi_{m+\delta}$, we can guarantee pseudo-thermalization once all the walks ($\delta = 0, 1, \dots, m$) have come sufficiently close to equilibrium. By properly taking into account the multiplicity of each δ , we derive the following upper bound on the m -th pseudo-thermalization time (see Appendix G):

$$t_{\text{PTherm}}^{(m)} \leq \tilde{O}(m^2 N^2), \quad (44)$$

where \tilde{O} indicates an upper bound up to logarithmic factors. Again, this is conditional on Conjecture 1.

Based on these bounds, summarized in Fig. 9(b), we can conclude that

- (i) at early times $t \leq \tilde{O}(N^2, mN)$, the system *can* be efficiently distinguished from Haar-random at the m -copy level.
- (ii) at late times $t \geq \tilde{\Omega}(m^2 N^2)$, the system *cannot* be efficiently distinguished from Haar-random at the m -copy level.

The nature of the crossover between these two regimes is an interesting open question, see Fig. 9(c). Under Conjecture 1, we have $t_{\text{mix}}^{(m)}/t_{\text{rel}}^{(m)} \rightarrow \infty$ in this limit for all m , suggestive of a cutoff phenomenon in the associated Markov chains $\Phi_{m\leftarrow K}[p_t]$. How would such cutoff phenomena be reflected in the quantum distinguishability measure Eq. (38)? Would the latter undergo an abrupt transition, would it decay gradually, or would it exhibit more complex behavior (e.g. a sequence of pre-cutoffs associated to each δ)? We leave this interesting question as a goal for future work.

VI. DISCUSSION

A. Summary

In this work, we discussed the dynamical generation and propagation of pseudoentanglement. We considered automaton circuits as models of dynamics that preserve the relevant ensembles of states: both the subset-phase states and the subset states, which have been introduced as “standard models” of pseudoentanglement in previous work [28, 29]. Specifically, we considered two models of automaton dynamics: an all-to-all interacting circuit, and a circuit of geometrically-local, 3-body, Toffoli-like gates on a d -dimensional qubit lattice (focusing mostly on $d = 1$). The all-to-all interacting model is exactly solvable, but the time scales for generation and propagation of pseudoentanglement are unphysically large (exponential in system size); the local circuit model does not suffer from these exponential time scales, but is less analytically tractable, so that our results are limited to a combination of rigorous bounds and conjectures supported by numerics.

We separately analyzed two related problems: the spreading of pseudoentanglement when a small pseudoentangled subsystem is placed in contact with a large trivial system, and the generation of pseudoentanglement starting from a product state. In both cases the key technical step involves mapping the problem onto the equilibration of certain classical random walks over subsets of the computational basis. This creates a connection to an interesting feature of Markov chains on highly-connected spaces: the cutoff phenomenon, whereby mixing happens in a step-like fashion in the limit of large system size, giving asymptotically sharp transitions to equilibrium. We argued that our Markov chains in many cases exhibit a cutoff phenomenon, giving sharp dynamical transitions in the distinguishability of our output states from Haar-random ones.

We named the dynamical approach toward pseudoentangled ensembles *pseudo-thermalization*, motivated by the analogy with the role of entanglement in quantum thermalization. This new concept adds to a growing body of research on the nuances of thermalization, chaos, ergodicity, scrambling, etc, that can be revealed only by higher-moment statistical quantities, thus going beyond the first- or second-moment quantities (e.g., local expectation values [65], out-of-time-ordered correlators [66]) that are traditionally the basis of such notions.

Other recently introduced ideas in this direction include *deep thermalization* [45, 46, 67–72], *complete Hilbert-space ergodicity* [19, 20], and thermalization via *free probability* or *cumulants* [47, 73]. However, those are stronger notions, based on information-theoretic (pseudo-)randomness of certain state ensembles generated for example by quantum measurements or by quasiperiodic drive sequences. The randomness can be quantified through the notion ϵ -approximate quantum state m -design, corresponding to the trace distance between moment operators being smaller than a tolerance ϵ (as in Eq. (2)); in those stronger versions of thermalization, one generally requires or expects an exponentially small tolerance $\epsilon \sim 1/\exp(N)$, or possibly even exact state designs ($\epsilon = 0$). For $m \geq 2$, these conditions imply high entanglement. Pseudo-thermalization in contrast is based on a computational notion of (pseudo-)randomness, where the observer is limited to polynomial resources (e.g. number of state copies) in their attempt to tell the states apart from truly random ones. Again in the language of state designs, this corresponds to a tolerance $\epsilon = o(1/\text{poly}(N))$ that is superpolynomially small (in order to trick the polynomially-bound observer), but not exponentially small, thus allowing for weakly entangled states.

B. Outlook

Our work opens a number of directions for future research. First of all, it would be desirable to improve and/or rigorize our results in several ways: by tighten-

ing bounds, especially on the mixing times in the local circuit model and on pseudothermalization without random phases; by proving or disproving our Conjecture 1 on the relaxation times in the local circuit model; and by proving the existence of cutoff phenomena in our Markov chains, for which we only showed a necessary condition (divergent ratio of mixing time and relaxation time). These improvements could have significant qualitative consequences on the physics. For example, one may hope to show that, in the local circuit model for pseudoentanglement spreading, Sec. IV C, the m -copy pseudothermalization transitions are sharply separated from one another, in the sense that the difference of consecutive mixing times $t_{\text{mix}}^{(m+1)} - t_{\text{mix}}^{(m)}$ is sufficiently larger than the relaxation time $t_{\text{rel}}^{(m)}$.

Another direction for future work is to identify physically realistic models of dynamics where pseudoentanglement is achieved in polynomial time. In the all-to-all model of Sec. IV B that time scale is exponential for trivial reasons; in the local model of Sec. IV C, the m -copy pseudothermalization time is polynomial in system size, but grows at least linearly with m , so that convergence to a pseudoentangled ensemble, indistinguishable from Haar-random with *any* polynomial number of copies $m = O(\text{poly}(N))$, requires super-polynomial time. This can be a mild super-polynomial scaling, e.g. $N^{\log N}$. Nonetheless it would be interesting to identify models of dynamics that generate pseudoentanglement in polynomial time. Such models cannot be random local automaton circuits, due to the counting bound, Eq. (30). Pseudorandom subset(-phase) state ensembles can be prepared efficiently by using quantum-secure pseudorandom permutations and phase functions [28]. In this work we have opted for truly random subsets, as these make for simpler models of circuit dynamics and are more in keeping with the spirit of quantum thermalization; it would be interesting to identify pseudorandom models of dynamics that can produce pseudoentanglement in polynomial time while maintaining a simple, “random-looking”, physically reasonable structure. A related construction of pseudorandom unitaries was recently shown to not be robust to perturbations [74], which might suggest intrinsic difficulties for this direction.

More broadly, subset(-phase) states are only one class

of pseudoentangled state ensembles. Due to their structure, these ensembles suggest automaton circuits as a natural models of dynamics. It would be interesting to identify different ensembles of pseudoentangled states and the types of quantum dynamics that might naturally produce them.

Recent works have introduced related notions of ‘pseudo-coherence’ [74], ‘pseudomagic’ [75], etc, which are analogous to pseudoentanglement but based on different resources (coherence, magic, etc). A natural extensions of our work would be to study the dynamics of other such pseudoresources in appropriate circuit models.

It is also interesting to ask whether, in analogy with measurement-induced entanglement phase transitions [76–79], one might obtain phase transitions in the dynamics of pseudoentanglement by enriching our automaton circuits with suitable projective measurements and other elements. For example, while the size of subsets is invariant under automaton gates, it generally decreases under Z measurements, and can increase under Hadamard gates and X measurements. Can the competition of these elements give rise to nontrivial phase transitions in the pseudoentanglement properties of late-time states?

Finally, the possible emergence of cutoff phenomena in pseudothermalization raises more general questions about the sharpness of thermalization in generic quantum dynamics. Are sharp transitions in distinguishability a generic feature of chaotic quantum dynamics [80, 81]? What are the right tools to analyze them? Can there particularly structured classes of time evolutions (e.g., with symmetry) exhibit different levels of sharpness? We leave these questions as an interesting target for future research.

ACKNOWLEDGMENTS

We thank Nick Hunter-Jones, Ethan Lake, and Scott Aaronson for stimulating discussions. We are especially grateful to Nick Hunter-Jones for pointing us to Ref. [61]. Some numerical simulations were carried out on HPC resources provided by the Texas Advanced Computing Center (TACC) at the University of Texas at Austin.

-
- [1] Ryszard Horodecki and Pawe Horodecki, “Quantum entanglement,” *Rev. Mod. Phys.* **81**, 865–942 (2009).
 - [2] Eric Chitambar and Gilad Gour, “Quantum resource theories,” *Reviews of Modern Physics* **91**, 025001 (2019).
 - [3] Alexei Kitaev and John Preskill, “Topological Entanglement Entropy,” *Physical Review Letters* **96**, 110404 (2006).
 - [4] Hui Li and F. D. M. Haldane, “Entanglement Spectrum as a Generalization of Entanglement Entropy: Identification of Topological Order in Non-Abelian Fractional Quantum Hall Effect States,” *Physical Review Letters* **101**, 010504 (2008).
 - [5] Hong-Chen Jiang, Zhenghan Wang, and Leon Balents, “Identifying topological order by entanglement entropy,” *Nature Physics* **8**, 902–905 (2012).
 - [6] Marcos Rigol, Vanja Dunjko, and Maxim Olshanii, “Thermalization and its mechanism for generic isolated quantum systems,” *Nature* **452**, 854–858 (2008).
 - [7] Rahul Nandkishore and David A. Huse, “Many-Body Localization and Thermalization in Quantum Statistical Mechanics,” *Annual Review of Condensed Matter Physics* **6**, 15–38 (2015).

- [8] Adam M. Kaufman, M. Eric Tai, Alexander Lukin, Matthew Rispoli, Robert Schittko, Philipp M. Preiss, and Markus Greiner, “Quantum thermalization through entanglement in an isolated many-body system,” *Science* **353**, 794–800 (2016).
- [9] Mark Mezei and Wilke van der Schee, “Black Holes Often Saturate Entanglement Entropy the Fastest,” *Physical Review Letters* **124**, 201601 (2020).
- [10] Alvaro M. Alhambra, “Quantum many-body systems in thermal equilibrium,” (2022), [10.48550/arXiv.2204.08349](https://arxiv.org/abs/10.48550/arXiv.2204.08349).
- [11] Lev Vidmar and Marcos Rigol, “Generalized Gibbs ensemble in integrable lattice models,” *Journal of Statistical Mechanics: Theory and Experiment* **2016**, 064007 (2016).
- [12] Adam Nahum, Jonathan Ruhman, Sagar Vijay, and Jeongwan Haah, “Quantum Entanglement Growth under Random Unitary Dynamics,” *Physical Review X* **7**, 031016 (2017).
- [13] Bruno Bertini, Pavel Kos, and Tomaz Prosen, “Entanglement Spreading in a Minimal Model of Maximal Many-Body Quantum Chaos,” *Physical Review X* **9**, 021033 (2019).
- [14] Tianci Zhou and Adam Nahum, “Entanglement Membrane in Chaotic Many-Body Systems,” *Phys. Rev. X* **10**, 031066 (2020).
- [15] Fernando G. S. L. Brandao, Wissam Chemissany, Nicholas Hunter-Jones, Richard Kueng, and John Preskill, “Models of quantum complexity growth,” *PRX Quantum* **2**, 030316 (2021).
- [16] Matthew P. A. Fisher, Vedika Khemani, Adam Nahum, and Sagar Vijay, “Random Quantum Circuits,” *arXiv e-prints* (2022), [10.48550/arXiv.2207.14280](https://arxiv.org/abs/10.48550/arXiv.2207.14280).
- [17] Andrew C. Potter and Romain Vasseur, “Entanglement Dynamics in Hybrid Quantum Circuits,” in *Entanglement in Spin Chains: From Theory to Quantum Technology Applications*, Quantum Science and Technology, edited by Abolfazl Bayat, Sougato Bose, and Henrik Johannesson (Cham, 2022) pp. 211–249.
- [18] Shivan Mittal and Nicholas Hunter-Jones, “Local random quantum circuits form approximate designs on arbitrary architectures,” (2023), [10.48550/arXiv.2310.19355](https://arxiv.org/abs/10.48550/arXiv.2310.19355).
- [19] Saul Pilatowsky-Cameo, Ceren B. Dag, Wen Wei Ho, and Soonwon Choi, “Complete Hilbert-Space Ergodicity in Quantum Dynamics of Generalized Fibonacci Drives,” *Physical Review Letters* **131**, 250401 (2023).
- [20] Saul Pilatowsky-Cameo, Iman Marvian, Soonwon Choi, and Wen Wei Ho, “Hilbert-Space Ergodicity in Driven Quantum Systems: Obstructions and Designs,” (2024), [10.48550/arXiv.2402.06720](https://arxiv.org/abs/10.48550/arXiv.2402.06720).
- [21] Don N. Page, “Average entropy of a subsystem,” *Phys. Rev. Lett.* **71**, 1291–1294 (1993).
- [22] Luigi Amico, Rosario Fazio, Andreas Osterloh, and Vlatko Vedral, “Entanglement in many-body systems,” *Reviews of Modern Physics* **80**, 517–576 (2008).
- [23] Rajibul Islam, Ruichao Ma, Philipp M. Preiss, M. Eric Tai, Alexander Lukin, Matthew Rispoli, and Markus Greiner, “Measuring entanglement entropy in a quantum many-body system,” *Nature* **528**, 77–83 (2015).
- [24] A. Elben, B. Vermersch, M. Dalmonte, J. I. Cirac, and P. Zoller, “Renyi Entropies from Random Quenches in Atomic Hubbard and Spin Models,” *Physical Review Letters* **120**, 050406 (2018).
- [25] Tiff Brydges, Andreas Elben, Petar Jurcevic, Benoit Vermersch, Christine Maier, Ben P. Lanyon, Peter Zoller, Rainer Blatt, *et al.*, “Probing Renyi entanglement entropy via randomized measurements,” *Science* **364**, 260–263 (2019).
- [26] Hsin-Yuan Huang, Richard Kueng, and John Preskill, “Predicting many properties of a quantum system from very few measurements,” *Nature Physics* **16**, 1050–1057 (2020).
- [27] Andreas Elben, Steven T. Flammia, Hsin-Yuan Huang, Richard Kueng, John Preskill, Benoit Vermersch, and Peter Zoller, “The randomized measurement toolbox,” *Nature Reviews Physics* **5**, 9–24 (2023).
- [28] Scott Aaronson, Adam Bouland, Bill Fefferman, Soumik Ghosh, Umesh Vazirani, Chenyi Zhang, and Zixin Zhou, “Quantum Pseudoentanglement,” (2023), [10.48550/arXiv.2211.00747](https://arxiv.org/abs/10.48550/arXiv.2211.00747).
- [29] Tudor Giurgica-Tiron and Adam Bouland, “Pseudorandomness from Subset States,” (2023), [10.48550/arXiv.2312.09206](https://arxiv.org/abs/10.48550/arXiv.2312.09206).
- [30] Zhengfeng Ji, Yi-Kai Liu, and Fang Song, “Pseudorandom Quantum States,” in *Advances in Cryptology - CRYPTO 2018*, edited by Hovav Shacham and Alexandra Boldyreva (Cham, 2018) pp. 126–152.
- [31] Chuhan Lu, Minglong Qin, Fang Song, Penghui Yao, and Mingnan Zhao, “Quantum Pseudorandom Scramblers,” (2023), [10.48550/arXiv.2309.08941](https://arxiv.org/abs/10.48550/arXiv.2309.08941).
- [32] Mark Zhandry, “A Note on Quantum-Secure PRPs,” (2016), [10.48550/arXiv.1611.05564](https://arxiv.org/abs/10.48550/arXiv.1611.05564).
- [33] Sarang Gopalakrishnan, “Operator growth and eigenstate entanglement in an interacting integrable Floquet system,” *Physical Review B* **98**, 060302 (2018).
- [34] Jason Iaconis, Sagar Vijay, and Rahul Nandkishore, “Anomalous subdiffusion from subsystem symmetries,” *Physical Review B* **100**, 214301 (2019).
- [35] Jason Iaconis, “Quantum State Complexity in Computationally Tractable Quantum Circuits,” *PRX Quantum* **2**, 010329 (2021).
- [36] Katja Klobas, Bruno Bertini, and Lorenzo Piroli, “Exact Thermalization Dynamics in the “Rule 54” Quantum Cellular Automaton,” *Physical Review Letters* **126**, 160602 (2021).
- [37] Persi Diaconis and Mehrdad Shahshahani, “Generating a random permutation with random transpositions,” *Zeitschrift für Wahrscheinlichkeitstheorie und Verwandte Gebiete* **57**, 159–179 (1981).
- [38] P Diaconis, “The cutoff phenomenon in finite Markov chains,” *Proceedings of the National Academy of Sciences* **93**, 1659–1664 (1996).
- [39] Guan-Yu Chen and Laurent Saloff-Coste, “The cutoff phenomenon for ergodic Markov processes,” *Electronic Journal of Probability [electronic only]* **13**, 26–78 (2008).
- [40] Hubert Lacoïn and Remi Leblond, “Cutoff phenomenon for the simple exclusion process on the complete graph,” (2011), [10.48550/arXiv.1010.4866](https://arxiv.org/abs/10.48550/arXiv.1010.4866).
- [41] Joe P. Chen, “The cutoff profile for exclusion processes in any dimension,” (2021), [10.48550/arXiv.2106.03685](https://arxiv.org/abs/10.48550/arXiv.2106.03685).
- [42] David Aldous and Persi Diaconis, “Shuffling Cards and Stopping Times,” *The American Mathematical Monthly* **93**, 333–348 (1986).
- [43] Daniel A. Roberts and Beni Yoshida, “Chaos and complexity by design,” *Journal of High Energy Physics* **2017**, 121 (2017).
- [44] Nicholas Hunter-Jones, “Unitary designs from statistical mechanics in random quantum circuits,” (2019),

- 10.48550/arXiv.1905.12053.
- [45] Jordan S. Cotler, Daniel K. Mark, Hsin-Yuan Huang, Felipe Hernandez, Joonhee Choi, Adam L. Shaw, Manuel Endres, and Soonwon Choi, “Emergent Quantum State Designs from Individual Many-Body Wave Functions,” *PRX Quantum* **4**, 010311 (2023).
- [46] Matteo Ippoliti and Wen Wei Ho, “Solvable model of deep thermalization with distinct design times,” *Quantum* **6**, 886 (2022).
- [47] Michele Fava, Jorge Kurchan, and Silvia Pappalardi, “Designs via Free Probability,” (2023), 10.48550/arXiv.2308.06200.
- [48] Michael A Nielsen and Isaac L Chuang, *Quantum computation and quantum information* (Cambridge university press, 2010).
- [49] David A Levin and Yuval Peres, *Markov chains and mixing times*, Vol. 107 (American Mathematical Soc., 2017).
- [50] Shlomo Hoory, Nathan Linial, and Avi Wigderson, “Expander graphs and their applications,” *Bulletin of the American Mathematical Society* **43**, 439–561 (2006).
- [51] Yuval Peres, “ARCC workshop: Sharp thresholds for mixing times,” (2004), online notes from a workshop of the American Institute of Mathematics, transcribed by S. Goel, A. Nachmias, P. Ralph and D. Shah.
- [52] Pietro Caputo, Thomas M. Liggett, and Thomas Richthammer, “Proof of Aldous’ spectral gap conjecture,” *Journal of the American Mathematical Society* **23**, 831–851 (2010).
- [53] Pasquale Calabrese and John Cardy, “Evolution of entanglement entropy in one-dimensional systems,” *Journal of Statistical Mechanics: Theory and Experiment* **2005**, P04010 (2005).
- [54] Pasquale Calabrese and John Cardy, “Entanglement entropy and conformal field theory,” *Journal of Physics A: Mathematical and Theoretical* **42**, 504005 (2009).
- [55] Tomaž Prosen and Marko Žnidarič, “Matrix product simulations of non-equilibrium steady states of quantum spin chains,” *Journal of Statistical Mechanics: Theory and Experiment* **2009**, P02035 (2009).
- [56] Marko Znidaric, Bojan Zunkovic, and Tomaz Prosen, “Transport properties of a boundary-driven one-dimensional gas of spinless fermions,” *Physical Review E* **84**, 051115 (2011).
- [57] Alan Morningstar, Luis Colmenarez, Vedika Khemani, David J. Luitz, and David A. Huse, “Avalanches and many-body resonances in many-body localized systems,” *Physical Review B* **105**, 174205 (2022).
- [58] Dries Sels, “Bath-induced delocalization in interacting disordered spin chains,” *Physical Review B* **106**, L020202 (2022).
- [59] Jonathan Hermon and Richard Pymar, “The exclusion process mixes (almost) faster than independent particles,” (2020), 10.48550/arXiv.1808.10846.
- [60] Persi Diaconis, R. L. Graham, and J. A. Morrison, “Asymptotic analysis of a random walk on a hypercube with many dimensions,” *Random Structures & Algorithms* **1**, 51–72 (1990).
- [61] W. T. Gowers, “An Almost m -wise Independent Random Permutation of the Cube,” *Combinatorics, Probability and Computing* **5**, 119–130 (1996).
- [62] Shlomo Hoory, Avner Magen, Steven Myers, and Charles Rackoff, “Simple permutations mix well,” *Theoretical Computer Science Automata, Languages and Programming: Algorithms and Complexity (ICALP-A 2004)*, **348**, 251–261 (2005).
- [63] Alex Brodsky and Shlomo Hoory, “Simple permutations mix even better,” *Random Structures & Algorithms* **32**, 274–289 (2008).
- [64] Daniel Jerison, “General mixing time bounds for finite Markov chains via the absolute spectral gap,” (2013), 10.48550/arXiv.1310.8021.
- [65] Mark Srednicki, “Chaos and quantum thermalization,” *Physical Review E* **50**, 888–901 (1994).
- [66] C. W. von Keyserlingk, Tibor Rakovszky, Frank Pollmann, and S. L. Sondhi, “Operator Hydrodynamics, OTOCs, and Entanglement Growth in Systems without Conservation Laws,” *Phys. Rev. X* **8**, 021013 (2018).
- [67] Wen Wei Ho and Soonwon Choi, “Exact Emergent Quantum State Designs from Quantum Chaotic Dynamics,” *Physical Review Letters* **128**, 060601 (2022).
- [68] Matteo Ippoliti and Wen Wei Ho, “Dynamical Purification and the Emergence of Quantum State Designs from the Projected Ensemble,” *PRX Quantum* **4**, 030322 (2023).
- [69] Maxime Lucas, Lorenzo Piroli, Jacopo De Nardis, and Andrea De Luca, “Generalized deep thermalization for free fermions,” *Physical Review A* **107**, 032215 (2023).
- [70] Tanmay Bhore, Jean-Yves Desaulles, and Zlatko Papić, “Deep thermalization in constrained quantum systems,” (2023), 10.48550/arXiv.2307.03769.
- [71] Harshank Shrotriya and Wen Wei Ho, “Non-locality of Deep Thermalization,” (2023), 10.48550/arXiv.2305.08437.
- [72] Amos Chan and Andrea De Luca, “Projected state ensemble of a generic model of many-body quantum chaos,” (2024).
- [73] Silvia Pappalardi, Felix Fritzsche, and Tomaz Prosen, “General Eigenstate Thermalization via Free Cumulants in Quantum Lattice Systems,” (2023), 10.48550/arXiv.2303.00713.
- [74] Tobias Haug, Kishor Bharti, and Dax Enshan Koh, “Pseudorandom unitaries are neither real nor sparse nor noise-robust,” (2023), 10.48550/arXiv.2306.11677.
- [75] Andi Gu, Lorenzo Leone, Soumik Ghosh, Jens Eisert, Susanne Yelin, and Yihui Quek, “A little magic means a lot,” (2023), 10.48550/arXiv.2308.16228.
- [76] Yaodong Li, Xiao Chen, and Matthew P. A. Fisher, “Quantum Zeno effect and the many-body entanglement transition,” *Physical Review B* **98**, 205136 (2018).
- [77] Brian Skinner, Jonathan Ruhman, and Adam Nahum, “Measurement-Induced Phase Transitions in the Dynamics of Entanglement,” *Physical Review X* **9**, 031009 (2019).
- [78] Michael J. Gullans and David A. Huse, “Dynamical Purification Phase Transition Induced by Quantum Measurements,” *Physical Review X* **10**, 041020 (2020).
- [79] Jason Iaconis, Andrew Lucas, and Xiao Chen, “Measurement-induced phase transitions in quantum automaton circuits,” *Physical Review B* **102**, 224311 (2020).
- [80] Michael J. Kastoryano, David Reeb, and Michael M. Wolf, “A Cutoff Phenomenon for Quantum Markov Chains,” *Journal of Physics A: Mathematical and Theoretical* **45**, 075307 (2012).
- [81] Sangchul Oh and Sabre Kais, “Cutoff phenomenon and entropic uncertainty for random quantum circuits,” *Electronic Structure* **5**, 035004 (2023).
- [82] V.V. Shende, A.K. Prasad, I.L. Markov, and J.P. Hayes,

“Synthesis of reversible logic circuits,” *IEEE Transactions on Computer-Aided Design of Integrated Circuits and Systems* **22**, 710–722 (2003).

- [83] Scott Aaronson, Daniel Grier, and Luke Schaeffer, “The Classification of Reversible Bit Operations,” (2015), 10.48550/arXiv.1504.05155.
- [84] Sabee Grewal, Vishnu Iyer, William Kretschmer, and Daniel Liang, “Low-Stabilizer-Complexity Quantum States Are Not Pseudorandom,” in *14th Innovations in Theoretical Computer Science Conference (ITCS 2023)*, Leibniz International Proceedings in Informatics (LIPIcs), Vol. 251, edited by Yael Tauman Kalai (Schloss Dagstuhl – Leibniz-Zentrum für Informatik, Dagstuhl, Germany, 2023) pp. 64:1–64:20.

Appendix A: Proof of Proposition 1

Here we prove Proposition 1 by analyzing the trace distance

$$\left\| \rho_{\mathcal{E}_p}^{(m)} - \rho_{\text{Haar}}^{(m)} \right\|_{\text{tr}} \quad (\text{A1})$$

between the m -th moment operators for the subset-phase ensemble \mathcal{E}_p (with uniformly random phases but arbitrarily-distributed subsets, $S \sim p$) and the Haar ensemble.

1. Preliminaries

In this Appendix we will denote computational basis states by integers $z \in [D] = \{0, 1, \dots, D-1\}$ rather than by bitstrings $\mathbf{z} \in \{0, 1\}^D$. We will reserve the latter notation for tuples of computational basis states, which are used later.

Eq. (A1) takes place within the symmetric sector of the m -fold replicated Hilbert space $\mathcal{H}^{\otimes m}$. It is thus helpful to introduce an orthonormal basis of that subspace:

$$|\mathbf{T}\rangle \equiv \binom{m}{\mathbf{T}}^{-1/2} \sum_{\mathbf{z}: \text{type}(\mathbf{z})=\mathbf{T}} |\mathbf{z}\rangle, \quad (\text{A2})$$

where $\mathbf{z} \in [D]^m$ is an m -tuple of basis states and $\text{type}(\mathbf{z}) \in [m+1]^D$ is a vector that counts the multiplicity of each basis state z in the m -tuple \mathbf{z} (the notation is borrowed from Ref. [28]): i.e., if $\text{type}(\mathbf{z}) = \mathbf{T}$, then T_i is the number of times the basis state $i \in [D]$ appears in \mathbf{z} . As a consequence we have $\sum_i T_i = m$. Finally, we used a shorthand for the multinomial coefficient

$$\binom{m}{\mathbf{T}} = \frac{m!}{T_0! \cdots T_{D-1}!}.$$

Types that consist only of 0’s and 1’s are called “unique types”. These describe non-degenerate m -tuples \mathbf{z} , where all elements are distinct. As such, unique types are equivalent to subsets of cardinality m : $\mathbf{T} \leftrightarrow S = \{z : T_z = 1\}$. With slight abuse of notation we will denote a unique-type state $|\mathbf{T}\rangle$ by the corresponding subset, $|S\rangle$.

We may write the Haar ensemble’s moment in terms of type states as

$$\rho_{\text{Haar}}^{(m)} = \binom{D+m-1}{m}^{-1} \sum_{\mathbf{T} \in \text{types}} |\mathbf{T}\rangle \langle \mathbf{T}|. \quad (\text{A3})$$

Further, it is useful to introduce the “unique-type state”

$$\begin{aligned} \rho_{\text{unique}}^{(m)} &= \binom{D}{m}^{-1} \sum_{\mathbf{T} \in \text{unique types}} |\mathbf{T}\rangle \langle \mathbf{T}| \\ &= \binom{D}{m}^{-1} \sum_{S' \in \Sigma_m} |S'\rangle \langle S'|. \end{aligned} \quad (\text{A4})$$

It is easy to verify that, as $D \rightarrow \infty$ with finite m , most types become unique, and $\rho_{\text{Haar}}^{(m)} \simeq \rho_{\text{unique}}^{(m)}$. We also introduce the same object restricted to basis states within a particular subset $S \in \Sigma_K$:

$$\rho_{S,\text{unique}}^{(m)} = \binom{K}{m}^{-1} \sum_{S' \in \Sigma_m: S' \subset S} |S'\rangle\langle S'|. \quad (\text{A5})$$

2. Proof

Our proof builds on Ref. [28], specifically the two facts below:

Fact A.1. *We have*

$$\left\| \rho_{\text{Haar}}^{(m)} - \sum_{S \in \Sigma_K} \pi_K(S) \rho_{S,\text{unique}}^{(m)} \right\|_{\text{tr}} \leq O\left(\frac{m^2}{K}\right),$$

with $\pi_K(S) = \binom{D}{K}^{-1}$ the uniform distribution on Σ_K .

Proof. See Proposition 2.3 in Ref. [28]. \square

Fact A.2. *We have*

$$\left\| \rho_{\mathcal{E}_p}^{(m)} - \sum_{S \in \Sigma_K} p(S) \rho_{S,\text{unique}}^{(m)} \right\|_{\text{tr}} \leq O\left(\frac{m^2}{K}\right),$$

Proof. See Proposition 2.4 in Ref. [28]. \square

By using these two facts and the triangle inequality, we can rephrase the LHS of Eq. (A1) as

$$\begin{aligned} \left\| \rho_{\mathcal{E}_p}^{(m)} - \rho_{\text{Haar}}^{(m)} \right\|_{\text{tr}} &= \left\| \sum_{S \in \Sigma_K} (p(S) - \pi_K(S)) \rho_{S,\text{unique}}^{(m)} \right\|_{\text{tr}} \\ &+ O\left(\frac{m^2}{K}\right). \end{aligned} \quad (\text{A6})$$

Now, using the definition of unique-type state Eq. (A5) and orthonormality of the unique-type states, we arrive at

$$\left\| \rho_{\mathcal{E}_p}^{(m)} - \rho_{\text{Haar}}^{(m)} \right\|_{\text{tr}} = \sum_{S' \in \Sigma_m} |f(S')| + O\left(\frac{m^2}{K}\right), \quad (\text{A7})$$

$$f(S') = \binom{K}{m}^{-1} \sum_{\substack{S \in \Sigma_K: \\ S' \subset S}} [p(S) - \pi_K(S)] \quad (\text{A8})$$

Finally, we obtain the statement of Proposition 1 by introducing the map $\Phi_{K \leftarrow m}$ of Eq. (16).

Appendix B: Properties of the Φ maps

Here we briefly analyze and prove some properties of the Φ maps.

Fact B.1. $\Phi_{m \leftarrow K}$ maps probability distributions on Σ_K to probability distributions on Σ_m .

Proof. It is straightforward to verify that $\Phi_{m \leftarrow K}[p]$ corresponds to the distribution on Σ_m obtained by composing these two processes: (i) draw $S \in \Sigma_K$ according to p ; (ii) draw (without replacement) m elements from S uniformly at random. \square

Fact B.2. *The maps Φ define a semigroup:*

$$\Phi_{c \leftarrow b} \circ \Phi_{b \leftarrow a} = \Phi_{c \leftarrow a} \quad (\text{B1})$$

for all $D \geq a > b > c \geq 1$.

Proof. We have

$$\begin{aligned} \Phi_{c \leftarrow b} \circ \Phi_{b \leftarrow a}[p](S'') &= \binom{a}{b}^{-1} \binom{b}{c}^{-1} \sum_{\substack{S, S': \\ S'' \subset S' \subset S}} p(S) \\ &= \binom{a}{b}^{-1} \binom{b}{c}^{-1} \binom{a-c}{b-c} \binom{a}{c} \\ &\quad \times \Phi_{c \leftarrow a}[p](S''), \end{aligned} \quad (\text{B2})$$

where in the second line we carried out the summation over S' (the c elements of $S' \cap S''$ are fixed, whereas the $b-c$ elements of $S' \setminus S''$ must be chosen from $S \setminus S''$, which has $a-c$ elements). Straightforward algebra shows the product of binomial coefficients is 1. Alternatively, without algebra, one can note that, given a set S with $|S| = a$, the following two processes are equivalent: (i) draw a uniformly-random subset $S' \subset S$ with $|S'| = b$, and then draw a uniformly-random subset $S'' \subset S'$ with $|S''| = c$; (ii) draw a uniformly-random subset $S'' \subset S$ with $|S''| = c$. \square

Next we focus on the relationship between the distributions $\Phi_{m \leftarrow K}[p]$ with different values of m . Let us consider the relevant situation of a random walk on the permutation group \mathcal{S}_D , represented by a probability distribution $\mathbb{P}_t(\sigma)$. This induces random walks on the spaces Σ_m for all m : picking an initial subset $S_0 \in \Sigma_m$, we can define

$$p_{t,S_0}^{(m)}(S) = \sum_{\sigma \in \mathcal{S}_D: \sigma(S_0)=S} \mathbb{P}_t(\sigma), \quad (\text{B3})$$

with $\sigma(S_0)$ representing the action of permutations on subsets.

Fact B.3. *Given a Markov chain $p_{t,S_0}^{(K)}(S)$ on Σ_K induced by a random walk on permutations as in Eq. (B3), we have*

$$\Phi_{m \leftarrow K} \left[p_{t,S_0}^{(K)} \right] (S') = \mathbb{E}_{S'_0} \left[p_{t,S'_0}^{(m)}(S') \right], \quad (\text{B4})$$

where the average is taken over subsets $S'_0 \in \Sigma_m$, $S'_0 \subset S_0$, according to the uniform measure.

Proof. Plugging in the definition of Φ , the LHS of Eq. (B4) reads

$$\begin{aligned}\Phi_{m \leftarrow K} [p_{t,S_0}^{(K)}] (S') &= \binom{K}{m}^{-1} \sum_{S: S' \subset S} p_{t,S_0}^{(K)}(S) \\ &= \binom{K}{m}^{-1} \sum_{S: S' \subset S} \sum_{\substack{\sigma \in \mathcal{S}_D: \\ \sigma(S_0)=S}} \mathbb{P}_t(\sigma) \\ &= \binom{K}{m}^{-1} \sum_{\substack{\sigma \in \mathcal{S}_D: \\ S' \subset \sigma(S_0)}} \mathbb{P}_t(\sigma). \quad (\text{B5})\end{aligned}$$

But the condition $S' \subset \sigma(S_0)$ is verified if and only if $S' = \sigma(S'_0)$ for some subset $S'_0 \subset S_0$. We therefore obtain

$$\begin{aligned}\Phi_{m \leftarrow K} [p_{t,S_0}^{(K)}] (S') &= \binom{K}{m}^{-1} \sum_{S'_0 \subset S_0} \sum_{\substack{\sigma \in \mathcal{S}_D: \\ S' = \sigma(S'_0)}} \mathbb{P}_t(\sigma) \\ &= \binom{K}{m}^{-1} \sum_{S'_0 \subset S_0} p_{t,S'_0}^{(m)}(S') \quad (\text{B6})\end{aligned}$$

where we have recognized the definition of $p_{t,S'_0}^{(m)}(S')$, the Markov chain induced on Σ_m , with initial state S'_0 averaged uniformly over all subsets of S_0 of the appropriate cardinality, as in Eq. (B4). \square

Fact B.4 (monotonicity). *The total variation distances*

$$\Delta_m \equiv \|\Phi_{m \leftarrow K}[p] - \pi_m\|_{\text{tv}} \quad (\text{B7})$$

are non-increasing in m .

Proof. We have

$$\begin{aligned}\Delta_{m-1} &= \|\Phi_{m-1 \leftarrow K}[p - \pi_K]\|_{\text{tv}} \\ &= \|\Phi_{m-1 \leftarrow K} \circ \Phi_{m \leftarrow K}[p - \pi_K]\|_{\text{tv}} \\ &\leq \|\Phi_{m \leftarrow K}[p - \pi_K]\|_{\text{tv}} = \Delta_m. \quad (\text{B8})\end{aligned}$$

The first line uses the fact that $\Phi_{m \leftarrow K}[\pi_K] = \pi_m$ for all $m < K$; the second uses the semigroup law of Φ maps, Fact B.2; the last one uses monotonicity of total variation norm under stochastic maps: $\|\Phi[\dots]\|_{\text{tv}} \leq \|\dots\|_{\text{tv}}$. \square

Appendix C: Proof of Proposition 2

We begin by recalling a useful fact proven in Ref. [29]:

Fact C.1. *For $\omega(\text{poly}(N)) < K < o(2^N)$, we have*

$$\left\| \sum_{S \in \Sigma_K} \pi_K(S) |\psi_S\rangle\langle\psi_S|^{\otimes m} - \rho_{\text{Haar}}^{(m)} \right\|_{\text{tr}} \leq O\left(\frac{mK}{D}, \frac{m^2}{K}\right). \quad (\text{C1})$$

Proof. See Theorem 1 in Ref. [29]. \square

Using this fact, in the relevant range of K , we can recast the LHS of Proposition 2 in the more convenient form

$$\left\| \sum_S [p(S) - \pi_K(S)] |\psi_S\rangle\langle\psi_S|^{\otimes m} \right\|_{\text{tr}} \quad (\text{C2})$$

up to small error $O(mK/D, m^2/K)$.

Next, using the type-state basis introduced in Appendix A, Eq. (A2), we can express the tensor power $|\psi_S\rangle^{\otimes m}$ as

$$|\psi_S\rangle^{\otimes m} = \frac{1}{K^{m/2}} \sum_{\mathbf{T} \in \mathcal{T}_S^m} \binom{m}{\mathbf{T}}^{1/2} |\mathbf{T}\rangle. \quad (\text{C3})$$

Here we use \mathcal{T}_S^m to represent all types of m -tuples that have nonzero components only for states in S . We also define pure *unique-type* states by

$$|\psi_{S,\text{uni}}^{(m)}\rangle = \binom{K}{m}^{-1/2} \sum_{S' \in \Sigma_m: S' \subset S} |S'\rangle, \quad (\text{C4})$$

where $|S'\rangle$ represents the unique-type basis state $|\mathbf{T}\rangle$ with 1's only on states in S' . As also noted in Appendix A, in the limit of $D \gg m$ most types are unique. This is helpful as it allows us to replace the state $|\psi_S\rangle$ in Eq. (C2) by its unique-type counterpart, $|\psi_{S,\text{uni}}\rangle$, with a small error. To show this, we first need a simple fact about the trace distance between pure states:

Fact C.2. *For any two pure states $|\phi\rangle, |\chi\rangle$ we have*

$$\| |\phi\rangle\langle\phi| - |\chi\rangle\langle\chi| \|_{\text{tr}} = 2\sqrt{1 - |\langle\phi|\chi\rangle|^2}. \quad (\text{C5})$$

Proof. See Fact 2 in Ref. [28] (set $\rho_1 = |\phi\rangle\langle\phi|$, $\rho_2 = |\chi\rangle\langle\chi|$). \square

We can now show the following:

Lemma C.1 (unique types suffice). *We have*

$$\left\| |\psi_S\rangle\langle\psi_S|^{\otimes m} - |\psi_{S,\text{uni}}^{(m)}\rangle\langle\psi_{S,\text{uni}}^{(m)}| \right\|_{\text{tr}} \leq O\left(\frac{m}{\sqrt{K}}\right). \quad (\text{C6})$$

Proof. Using Fact C.2, the LHS reads

$$2\sqrt{1 - \left| \langle\psi_S^{\otimes m} | \psi_{S,\text{uni}}^{(m)}\rangle \right|^2}.$$

Writing both $|\psi_S^{\otimes m}\rangle$ and $|\psi_{S,\text{uni}}^{(m)}\rangle$ in their type basis representation, we get the inner product

$$\begin{aligned}\langle\psi_S^{\otimes m} | \psi_{S,\text{uni}}^{(m)}\rangle &= K^{-m/2} \binom{K}{m}^{-1/2} \\ &\quad \times \sum_{\mathbf{T} \in \mathcal{T}_S^m} \binom{m}{\mathbf{T}}^{1/2} \delta(\mathbf{T} \text{ is unique}) \\ &= (m!)^{1/2} K^{-m/2} \binom{K}{m}^{1/2}. \quad (\text{C7})\end{aligned}$$

Using some straightforward algebra and the ‘birthday asymptotics’ $\frac{K!}{(K-m)!} = K^m (1 + O(m^2/K))$ (see e.g. Fact 1 in Ref. [29]) we finally get

$$\sqrt{1 - \left| \langle \psi_S^{\otimes m} | \psi_{S,\text{uni}}^{(m)} \rangle \right|^2} = O\left(\frac{m}{\sqrt{K}}\right). \quad (\text{C8})$$

□

Putting it all together, we can rewrite Eq. (C2) as

$$\left\| \sum_{S \in \Sigma_K} (p(S) - \pi_K(S)) \left| \psi_{S,\text{uni}}^{(m)} \right\rangle \left\langle \psi_{S,\text{uni}}^{(m)} \right| \right\|_{\text{tr}} \quad (\text{C9})$$

now up to error $O(m/\sqrt{K})$. Finally, plugging in the definition of unique-type pure states, Eq. (C4), yields

$$\begin{aligned} & \left\| \sum_{S \in \Sigma_K} (p(S) - \pi_K(S)) \binom{K}{m}^{-1} \sum_{\substack{S', S'' \in \Sigma_m: \\ S', S'' \subset S}} |S'\rangle\langle S''| \right\|_{\text{tr}} \\ &= \left\| \sum_{S', S'' \in \Sigma_m} |S'\rangle\langle S''| \binom{K}{m}^{-1} \sum_{\substack{S \in \Sigma_K: \\ S' \cup S'' \subset S}} (p(S) - \pi_K(S)) \right\|_{\text{tr}}. \end{aligned} \quad (\text{C10})$$

We can recognize the coefficient of $|S'\rangle\langle S''|$ as

$$\binom{K}{m}^{-1} \binom{K}{m+\delta} \Phi_{m+\delta \leftarrow K} [p - \pi](S' \cup S'') \quad (\text{C11})$$

which is the matrix $\mathcal{M}_p^{(m)}$ in Proposition 2.

Appendix D: Random walk on the hypercube

1. Single particle

In this Appendix we review, for completeness, the solution of the simple random walk on the hypercube \mathbb{Z}_2^N [60]. We label each vertex of the hypercube by a bitstring $\mathbf{z} \in \{0, 1\}^N$; two vertices \mathbf{x}, \mathbf{y} are neighbors iff the corresponding bitstrings have Hamming distance 1: $|\mathbf{x} \oplus \mathbf{y}'| = 1$ (\oplus is sum modulo 2). In each time step the walker hops randomly in any one of the N directions, represented by the Markov chain transition matrix

$$\Gamma_{\mathbf{x}, \mathbf{y}} = \frac{1}{N} \delta_{|\mathbf{x} \oplus \mathbf{y}|, 1}. \quad (\text{D1})$$

Note that as written, the walk is not aperiodic: the parity of the Hamming weight alternates in each time step (i.e., the hypercube is bipartite). This problem can be eliminated by allowing idling, i.e. replacing $\Gamma_{\mathbf{x}, \mathbf{y}} \mapsto p\Gamma_{\mathbf{x}, \mathbf{y}} + (1-p)\delta_{\mathbf{x}, \mathbf{y}}$ (the walker takes a step with probability p , remains in place otherwise). This does not

change the eigenfunctions and changes the eigenvalues in a trivial way, $\lambda \mapsto p\lambda + (1-p)$.

The transition matrix in Eq. (D1) is diagonalized via the Hadamard transform, $H_{\mathbf{a}, \mathbf{x}} \equiv \frac{1}{\sqrt{D}} (-1)^{\mathbf{a} \cdot \mathbf{x}}$:

$$\begin{aligned} \tilde{\Gamma}_{\mathbf{a}, \mathbf{b}} &\equiv \frac{1}{D} \sum_{\mathbf{x}, \mathbf{y}} \Gamma_{\mathbf{x}, \mathbf{y}} (-1)^{\mathbf{a} \cdot \mathbf{x} + \mathbf{b} \cdot \mathbf{y}} \\ &= \frac{1}{ND} \sum_{\mathbf{x}, \mathbf{r}} \delta_{|\mathbf{r}|, 1} (-1)^{(\mathbf{a} \oplus \mathbf{b}) \cdot \mathbf{x} + \mathbf{b} \cdot \mathbf{r}} \\ &= \delta_{\mathbf{a}, \mathbf{b}} \frac{1}{N} \sum_{i=1}^N (-1)^{b_i} \equiv \delta_{\mathbf{a}, \mathbf{b}} \lambda_{\mathbf{a}}. \end{aligned} \quad (\text{D2})$$

Here we have introduced $\mathbf{r} \equiv \mathbf{x} \oplus \mathbf{y}$ and used $\sum_{\mathbf{x}} (-1)^{\mathbf{x} \cdot \mathbf{c}} = D \delta_{\mathbf{c}, \mathbf{0}}$. The eigenvalue associated to ‘‘wave vector’’ $\mathbf{a} \in \{0, 1\}^N$ is

$$\lambda_{\mathbf{a}} = \frac{1}{N} \sum_{i=1}^N (1 - 2a_i) = 1 - 2 \frac{|\mathbf{a}|}{N}, \quad (\text{D3})$$

which is only a function of Hamming weight $|\mathbf{a}|$.

There is a non-degenerate $\lambda_0 = 1$ eigenvalue, associated to $\mathbf{a} = \mathbf{0}$ (the uniform state), then a gap of magnitude $2/N$, and then an N -fold degenerate eigenvalue $\lambda_1 = 1 - 2/N$. The relaxation time is therefore $t_{\text{rel}} = 1/(1 - \lambda_1) = N/2$. One can also identify the mixing time exactly and prove that the problem (with idling) features a cutoff [60]. A simple way to estimate the mixing time is to require that $N\lambda_1^t$ be small, which gives $t_{\text{mix}} \sim N \log(N)$ (the correct scaling up to constant factors).

The gate set of Sec. IV C induces a simple random walk on the hypercube with idling parameter $p = 1/4$, giving rescaled eigenvalues $\lambda_1 = 1 - \frac{2}{N} \mapsto \frac{1}{4}\lambda_1 + \frac{3}{4} = 1 - \frac{1}{2N}$, thus the relaxation time $t_{\text{rel}} = 2N$.

2. Many particles: multipole eigenmodes

The eigenvalues $\lambda_{\mathbf{a}}$, Eq. (D3), also appear in the spectra of the Markov chains with $m > 1$. We can construct the corresponding eigenmodes directly. Let us introduce the functions

$$f_{\mathbf{a}}(S) = \frac{n_S(Z_{\mathbf{a}} = +1) - n_S(Z_{\mathbf{a}} = -1)}{m}, \quad (\text{D4})$$

where for each bitstring $\mathbf{a} \in \mathbb{Z}_2^N$ we defined $Z_{\mathbf{a}} = \bigotimes_{i=1}^N Z_i^{a_i}$, and $n_S(Z_{\mathbf{a}} = \pm 1)$ is the number of elements $\mathbf{z} \in S$ such that $\langle \mathbf{z} | Z_{\mathbf{a}} | \mathbf{z} \rangle = \pm 1$. The action of the transition matrix $\Gamma_{S, S'}$ on these functions is:

$$\begin{aligned} \sum_{S'} \Gamma_{S, S'} f_{\mathbf{a}}(S') &= \sum_{S'} \frac{|\{u \in \mathcal{G} : uS = S'\}|}{|\mathcal{G}|} f_{\mathbf{a}}(S') \\ &= \sum_{u \in \mathcal{G}} \frac{1}{|\mathcal{G}|} f_{\mathbf{a}}(uS) \end{aligned} \quad (\text{D5})$$

Here we have used the definition of the transition probability $\Gamma_{S,S'}$ as the fraction of gates u in the gate set \mathcal{G} that maps subset S to S' , and then changed variables via $S' \equiv uS$. Summing over u over-counts each subset S' in the original sum by a factor of $|\{u' \in \mathcal{G} : u'S = uS\}|$, which precisely cancels the numerator in $\Gamma_{S,S'}$. Now we note that

$$f_{\mathbf{a}}(uS) \propto 1 - 2n_{uS}(Z_{\mathbf{a}} = -1) = 1 - 2n_S(uZ_{\mathbf{a}}u = -1). \quad (\text{D6})$$

If u is the CCX gate that flips qubit i controlled by its neighbors $i \pm 1$ being in states $c_{\pm} \in \{-1, 1\}$, we have

$$uZ_iu = \left[I - 2 \frac{I + c_+ Z_{i+1}}{2} \frac{I + c_- Z_{i-1}}{2} \right] Z_i \quad (\text{D7})$$

and $uZ_ju = Z_j$ for all $j \neq i$. The operator uZ_iu has eigenvalues ± 1 in equal numbers. The $+1$ eigenspace is specified by $Z_i = -1$ and $c_- Z_{i-1} = c_+ Z_{i+1} = +1$ ($D/8$ states), or $Z_i = +1$ and $c_{\xi} Z_{i+\xi} = -1$ for at least one $\xi \in \{-1, +1\}$ ($3D/8$ states). The remaining $D/2$ computational basis states form the -1 eigenspace. It is easy to see that each computational basis state with $Z_i = +1$ is in the $+1$ eigenspace of uZ_iu for 3 choices of control bits, and in the -1 eigenspace for one choice ($c_+ = c_- = +1$). Therefore, when we sum over the control bits $c_{\pm} \in \{0, 1\}$ (as part of our sum over $u \in \mathcal{G}$) we find $\sum_{c_{\pm}} n_S(u_{i,c_{\pm}} Z_{\mathbf{a}} u_{i,c_{\pm}} = +1) = (4 - 2\delta_{a_i,1}) n_S(Z_i = +1)$. On net, we find

$$\begin{aligned} \frac{1}{4N} \sum_{u \in \mathcal{G}} f_{\mathbf{a}}(uS) &= \frac{1}{4N} \sum_{i=1}^N \sum_{c_{\pm} = \pm 1} f_{\mathbf{a}}(u_{i,c_{\pm}} S) \\ &= \frac{1}{N} \sum_{i=1}^N \frac{4 - 2\delta_{a_i,1}}{4} f_{\mathbf{a}}(S) \\ &= \left(1 - \frac{|\mathbf{a}|}{2N} \right) f_{\mathbf{a}}(S) = \lambda_{\mathbf{a}} f_{\mathbf{a}}(S), \quad (\text{D8}) \end{aligned}$$

where we recognize the eigenvalue $\lambda_{\mathbf{a}}$ of the simple random walk (with $3/4$ idling probability).

These eigenmodes for the m -particle problem have an intuitive interpretation. $|\mathbf{a}| = 0$ represents a monopole moment (i.e. total particle number), which is conserved; $|\mathbf{a}| = 1$ yields the N components of the dipole moment, or center of mass position, which are the slowest decaying modes in the problem; $|\mathbf{a}| = 2$ yields the $\binom{N}{2}$ components of the quadrupole moment, which decay more quickly; and so on for higher multipole moments.

For $m = 1$ the $2^N \{f_{\mathbf{a}}\}$ modes exhaust the spectrum, whereas for $m \geq 2$ they make up only a small part. Still, they are very important, since they describe the decay of circuit-averaged expectation values $\overline{\langle Z_{\mathbf{a}} \rangle}$. Indeed, we have

$$\begin{aligned} \overline{\langle Z_{\mathbf{a}}(t) \rangle} &= \sum_S p_t(S) \langle \psi_S | Z_{\mathbf{a}} | \psi_S \rangle = (p_t | f_{\mathbf{a}}) \\ &= (p_0 | \Gamma^t | f_{\mathbf{a}}) = \left(1 - \frac{|\mathbf{a}|}{2N} \right)^t (p_0 | f_{\mathbf{a}}), \quad (\text{D9}) \end{aligned}$$

where we used the definition $\langle \psi_S | Z_{\mathbf{a}} | \psi_S \rangle = f_{\mathbf{a}}(S)$, introduced the inner product $(a|b) = \sum_S a(S)b(S)$ between real functions on Σ_m , and used the Hermiticity of the transition matrix Γ (reversibility of the Markov chain) to express the time-evolved probability distribution $(p_t | = (p_0 | \Gamma^t$.

It follows that any eigenmode $h(S)$ of the m -particle random walk whose eigenvalue is *not* in the single-particle spectrum does not show up in circuit-averaged expectation values $\overline{\langle Z_{\mathbf{a}} \rangle}$:

$$\sum_S h(S) \langle \psi_S | Z_{\mathbf{a}} | \psi_S \rangle = \sum_S h(S) f_{\mathbf{a}}(S) = (h | f_{\mathbf{a}}) = 0, \quad (\text{D10})$$

due to orthogonality of the eigenmodes (Hermiticity of Γ). Such eigenmodes instead can appear in correlation functions across circuit realizations, e.g. $\overline{\langle Z_{\mathbf{a}} \rangle \langle Z_{\mathbf{b}} \rangle}$.

3. Two particles: relative coordinate eigenmodes

Here we provide more details on eigenmodes of the two-particle problem that depend subset $S = \{\mathbf{z}, \mathbf{z}'\}$ only through the relative coordinate $\mathbf{r} = \mathbf{z} \oplus \mathbf{z}'$. Let us consider how \mathbf{r} might change under the action of our local automaton gate set $\mathcal{G} = \{u_{iab}\}$. There are two cases to consider:

- If $r_{i-1} = r_{i+1} = 0$ (i.e., $z_{i-1} = z'_{i-1}$ and $z_{i+1} = z'_{i+1}$), then either both z_i and z'_i flip, or neither one flips; either way, \mathbf{r} is unchanged.
- Otherwise, there is a $1/4$ probability (based on randomly drawn control bits a, b) that u_{iab} flips z_i but not z'_i , a $1/4$ probability that it flips z'_i but not z_i , and a $1/2$ probability that it flips neither. In all, there is a $1/2$ probability that r_i flips.

The rules above describe a random walk on \mathbb{Z}_2^N based on “activated” bit flips, where r_i can flip only if one of its neighbors $r_{i\pm 1}$ is 1. Clearly $\mathbf{r} = \mathbf{0}$ is a steady state, but it does not describe a valid subset (it gives $\mathbf{z} = \mathbf{z}'$). One can check that the restriction to $\mathbb{Z}_2^N \setminus \{\mathbf{0}\}$ is irreducible, aperiodic (since lazy moves are allowed) and reversible, thus it has the uniform distribution as unique steady state.

One can write down the transition matrix $\Gamma|_R$ for the relative coordinate as a quantum Hamiltonian:

$$\Gamma|_R = \frac{1}{N} \sum_{i=1}^N \left[(I - \Pi_i) \frac{I + X_i}{2} + \Pi_i \right] \equiv I - \frac{H}{N}, \quad (\text{D11})$$

$$\Pi_i = |0\rangle\langle 0|_{i-1} \otimes |0\rangle\langle 0|_{i+1} \otimes I_{\text{not } i\pm 1}. \quad (\text{D12})$$

The linear-in- N relaxation time corresponds to the Hamiltonian \mathcal{H} being gapped.

Appendix E: Properties of the local automaton gate set

In this Appendix we give more details on the local automaton gate set \mathcal{G} used in Sec. IV C. We recall that the gate set is defined as $\mathcal{G} = \{u_{iab} = C_{i-1,a}C_{i+1,b}X_i\}$, with $i \in [N]$, $a, b \in \{0, 1\}$, and periodic boundary conditions (i.e., $i \pm 1$ are taken modulo N). Each time step consists of drawing a gate $u_{iab} \in \mathcal{G}$ uniformly at random and applying it to the system. This defines a random walk on the permutation group \mathcal{S}_D with transition matrix

$$\Gamma_{\sigma, \sigma'} = \frac{1}{|\mathcal{G}|} \sum_{u \in \mathcal{G}} \delta_{\sigma', u \circ \sigma}, \quad (\text{E1})$$

where with slight abuse of notation we treat the gate u as a permutation of the computational basis. Through the natural action of permutations on subsets,

$$S \xrightarrow{\sigma} \{\sigma(i) : i \in S\} \equiv \sigma(S),$$

this also defines a Markov chain on the subset spaces Σ_m for each m , with transition matrices

$$\Gamma_{S, S'} = \frac{1}{|\mathcal{G}|} \sum_{u \in \mathcal{G}} \delta_{S', u(S)} \quad (\text{E2})$$

(we use Γ for all these transition matrices and rely on the indices to distinguish them).

To show that $\Gamma_{S, S'}$ equilibrates to the unique steady state π_m (the uniform distribution on Σ_m), we need the following three facts to hold:

Lemma E.1 (reversibility). *The Markov chain $\Gamma_{S, S'}$ on Σ_m is reversible for all m .*

Proof. Since the gate set \mathcal{G} is such that $u^2 = I$ for all $u \in \mathcal{G}$, we have $u(S) = S'$ if and only if $u(S') = S$. Thus $\Gamma_{S, S'} = \Gamma_{S', S}$ for all $S, S' \in \Sigma_m$. \square

Lemma E.2 (irreducibility). *The Markov chain $\Gamma_{S, S'}$ on Σ_m is irreducible for all $m \leq D - 2$.*

Proof. It is well known [82, 83] that the Toffoli (CCX) and NOT (X) gates are ‘‘almost’’ universal for classical computation, in the sense that they generate the subgroup of \mathcal{S}_D made of even permutations (permutations that can be decomposed into an even number of transpositions). Our gate set includes Toffoli gates between consecutive qubits (u_{i11}); further, it can generate NOT gates ($X_i = u_{i00}u_{i01}u_{i10}u_{i11}$) and CNOT gates between neighboring qubits, with either choice of control and target:

$$C_{i-1,a}X_i = u_{ia0}u_{ia1}, \quad C_{i+1,a}X_i = u_{i0a}u_{i1a}.$$

With the local CNOTs we can make a local SWAP gate:

$$\text{SWAP}_{i,i+1} = C_{i,0}X_{i+1} \circ C_{i+1,0}X_i \circ C_{i,0}X_{i+1}.$$

Finally, by composing local SWAPs we can make arbitrary permutations of the qubits, and thus generate the

whole (non-local) Toffoli + NOT gate set. Therefore \mathcal{G} generates all even permutations. Now, given two sets $S, S' \in \Sigma_m$, we can find a permutation $\sigma \in \mathcal{S}_D$ that maps one to the other: $S' = \sigma(S)$. If σ is even, we are done. If σ is odd, then let $i, j \in [D]$ be two basis states that are *not* in subset S (we have assumed $|S| = m \leq D - 2$ so that two such states exist), and let $\tau_{ij} \in \mathcal{S}_D$ be the transposition $i \leftrightarrow j$. Then $u \circ \tau_{ij}$ is an even permutation that maps S to S' . Since any two sets can be connected by an even permutation and any even permutation can be decomposed into a product of $u \in \mathcal{G}$, the Markov chain can connect any two subsets $S, S' \in \Sigma_m$ and is thus irreducible. \square

Lemma E.3 (aperiodicity). *The Markov chain $\Gamma_{S, S'}$ on Σ_m is aperiodic for any $m \leq D/4$.*

Proof. Given two sets $S, S' \in \Sigma_m$, we are going to show that the Markov chain can connect S to S' with paths of any length $l \geq l_{\min}$, with l_{\min} some finite integer. To do so, let us introduce a third state S'' with the property that all bitstrings $z \in S''$ have zeros at positions $i - 1$ and $i + 1$, for some i (this limits the size of the subset to $m \leq D/4$). Since the chain is irreducible, we can find a sequence of l_1 gates whose product maps S to S'' and another sequence of l_2 gates whose product maps S'' to S' . Then, inserting a gate u_{i11} between these two sequences ι times produces a path from S to S' of length $l_1 + \iota + l_2$. This can take any value larger than $l_{\min} \equiv l_1 + l_2$. \square

Reversibility, irreducibility and aperiodicity imply that the Markov chain has the uniform distribution π_m as its unique steady state [49]. This proves that our 3-qubit automaton gate set equilibrates to the uniform distribution on all subset states with $|S| = m \leq D/4$.

Furthermore, it is easy to see that three-qubit gates are necessary to obtain the above result. Indeed two-qubit automaton gates (generated by NOT and CNOT) are *affine transformations*, in the sense that for any such gate u we have $u|\mathbf{z}\rangle = |A_u\mathbf{z} \oplus \mathbf{b}_u\rangle$, with A_u a binary matrix and \mathbf{b}_u a bitstring. Any transformations that are not affine cannot be generated by two-qubit automaton gates. As it turns out, the gate set comprising NOT and CNOT gates satisfies irreducibility up to $m = 3$; an example of two subsets that cannot be connected with $m = 4$ and $N = 3$ is given by

$$S = \begin{bmatrix} 0 & 1 & 1 \\ 0 & 1 & 0 \\ 0 & 0 & 1 \\ 0 & 0 & 0 \end{bmatrix}, \quad S' = \begin{bmatrix} 1 & 0 & 0 \\ 0 & 1 & 0 \\ 0 & 0 & 1 \\ 0 & 0 & 0 \end{bmatrix} \quad (\text{E3})$$

(each row is a bitstring \mathbf{z} in the set). It is easy to see that the sum (modulo 2) of bitstrings in each set, \mathbf{z}_{tot} , transforms under automaton gate u according to $\mathbf{z}_{\text{tot}} \mapsto A_u\mathbf{z}_{\text{tot}}$ (the additive term \mathbf{b}_u appears 4 times and thus cancels). But S has $\mathbf{z}_{\text{tot}} = (0, 0, 0)$ while S' has $\mathbf{z}_{\text{tot}} = (1, 1, 1)$, so any sequence of u 's mapping S to S'

must be such that $\prod_u A_u$ annihilates $(1, 1, 1)$. This is incompatible with a reversible computation (e.g. it would imply a collision between strings 000 and 111).

Another way of arriving at a similar conclusion is that pseudoentanglement requires magic [84], and two-qubit automaton gate sets happen to also be Clifford. Thus if we start from a stabilizer subset state (e.g. $|0\rangle^{\otimes N-k} \otimes |+\rangle^{\otimes k}$) we cannot produce a pseudoentangled ensemble. However, for $m \leq 3$, it is instead possible to show that the gate set comprising NOT and CNOT yields irreducible Markov chains. This is perhaps related to the fact that mimicking the 3 lowest moments of the Haar measure does not require magic (as Clifford circuits form 3-designs on qubits).

Appendix F: Upper bound on relaxation time with local gate set

In Sec. IV C we study the relaxation time of the Markov chains induced by the local automaton gate set $\mathcal{G} = \{\mathcal{C}_{i-1,a}\mathcal{C}_{i+1,b}X_i\}$ and, based on numerical observations, we conjecture the scaling $t_{\text{rel}}^{(m)} = \Theta(N)$, independent of m (Conjecture 1). While the single-particle spectrum, solved analytically in App. D 1, gives a lower bound $t_{\text{rel}}^{(m)} \geq \Omega(N)$, an upper bound is harder to obtain analytically. Here we prove the upper bound

$$t_{\text{rel}}^{(m)} \leq O(mN^5). \quad (\text{F1})$$

We believe this is a very loose upper bound (again Conjecture 1 corresponds to $t_{\text{rel}}^{(m)} \leq O(N)$) and it would be interesting to identify different techniques to tighten it.

Our proof technique is based on the *comparison method* [49], which provides a bound

$$t_{\text{rel}} \leq B\tilde{t}_{\text{rel}} \quad (\text{F2})$$

on the relaxation time t_{rel} of a Markov chain Γ in terms of the relaxation time \tilde{t}_{rel} of another Markov chain $\tilde{\Gamma}$ on the same space. To define the coefficient B , we first need to introduce some background and notation. We consider a graph (V, E) with vertices V and edges E ; the reversible Markov chain Γ allows transitions between any two vertices connected by an edge, with probability $\Gamma_{e_1 e_2}$ where $(e_1, e_2) = e \in E$ denotes the edge. We also have another graph with the same vertices but different edges, (V, \tilde{E}) , with a Markov chain $\tilde{\Gamma}$ allowing transitions along the \tilde{E} edges. We assume that, for any edge $\tilde{e} = (x, y) \in \tilde{E}$ in the second graph, one can find a path γ_{xy} along the first graph (V, E) connecting x to y . $|\gamma_{xy}|$ denotes the length of that path. We say that $e \in \gamma_{xy}$ if the path traverses edge $e \in E$. With this notation in place, we can write down the expression for the coefficient B in the comparison bound:

$$B = \max_{e \in E} \frac{1}{\Gamma_{e_1 e_2}} \sum_{x, y: \gamma_{xy} \ni e} \tilde{\Gamma}_{xy} |\gamma_{xy}|. \quad (\text{F3})$$

Our strategy is to use our Markov chain (induced by the local automaton gate set \mathcal{G}) as Γ and use the Markov chain induced by ‘simple permutations’ [61, 62] as $\tilde{\Gamma}$. ‘Simple permutations’ are defined as the gate set $\tilde{\mathcal{G}} = \{v_{ijk, \sigma} : i, j, k \in [N], \sigma \in S_8\}$, where $v_{ijk, \sigma}$ acts as a 3-qubit automaton gate¹⁴ (associated to a permutation $\sigma \in S_8$) on qubits i, j, k . Note that the choice of qubits i, j, k is also arbitrary, in particular they need not be consecutive. So ‘simple permutations’ are 3-local but not geometrically local. ‘Simple permutations’ have been studied in the probability literature [61, 62] due to their good mixing properties, and several bounds on their relaxation and mixing times are known. For our purpose, we will need the following fact:

Fact F.1 (relaxation time from simple permutations). ‘Simple permutations’ $\tilde{\mathcal{G}}$ induce a Markov chain on Σ_m whose relaxation time is bounded above as

$$\tilde{t}_{\text{rel}}^{(m)} \leq O(mN^2). \quad (\text{F4})$$

Proof. Ref. [63] considers the random walk induced by ‘simple permutations’ on *ordered* m -tuples, $\mathbf{z} = (z_1, \dots, z_m)$, rather than sets $S = \{z_1, \dots, z_m\} \in \Sigma_m$. It shows that the former has relaxation time $\tilde{t}_{\text{rel}}^{(m, \text{ord.})} \leq O(mN^2)$. We will show that

$$\tilde{t}_{\text{rel}}^{(m)} \leq \tilde{t}_{\text{rel}}^{(m, \text{ord.})} \quad (\text{F5})$$

(the walk on ordered m -tuples relaxes no faster than that on subsets), which implies Eq. (F4).

Consider an eigenfunction f of the Markov chain on subsets:

$$\frac{1}{|\tilde{\mathcal{G}}|} \sum_{v \in \tilde{\mathcal{G}}} f(v(S)) = \lambda f(S). \quad (\text{F6})$$

Let us define a function g on the space of ordered m -tuples by setting $g(\mathbf{z}) = f(\text{set}(\mathbf{z}))$, where $\text{set}(\mathbf{z}) \in \Sigma_m$ is the *unordered* set of elements in the m -tuple \mathbf{z} . We can easily check that g is an eigenfunction of the Markov chain on ordered m -tuples with the same eigenvalue λ :

$$\begin{aligned} \frac{1}{|\tilde{\mathcal{G}}|} \sum_{v \in \tilde{\mathcal{G}}} g(v(\mathbf{z})) &= \frac{1}{|\tilde{\mathcal{G}}|} \sum_{v \in \tilde{\mathcal{G}}} f(\text{set}(v(\mathbf{z}))) \\ &= \frac{1}{|\tilde{\mathcal{G}}|} \sum_{v \in \tilde{\mathcal{G}}} f(v(\text{set}(\mathbf{z}))) \\ &= \lambda f(\text{set}(\mathbf{z})) = \lambda g(\mathbf{z}). \end{aligned} \quad (\text{F7})$$

Thus the spectrum of the Markov chain on subsets is included within the spectrum of the Markov chain on ordered tuples. Recalling that the relaxation time is the inverse spectral gap, Eq. (F5) follows. \square

¹⁴ In ‘width-2’ simple permutations [62, 63], which we use here to establish our upper bound, σ is restricted to act as a flip of bit i controlled by an arbitrary Boolean function of bits j, k . The Toffoli gate falls in this category, with the Boolean function being AND.

Now that we have an upper bound on $\tilde{t}_{\text{rel}}^{(m)}$, it remains to upper-bound the coefficient B in the comparison bound, Eq. (F3). We break it down into three bounds:

Fact F.2. For any edge $e \in E$, we have

$$\frac{1}{\Gamma_e} \leq O(N). \quad (\text{F8})$$

Proof. Follows from the fact that $\Gamma_{S,S'} \geq 1/|\mathcal{G}| = \frac{1}{4N}$ (at least one gate $u \in \mathcal{G}$ must connect S to S'). \square

Fact F.3. For any two subsets S, S' we have

$$|\gamma_{S,S'}| \leq O(N). \quad (\text{F9})$$

Proof. For any two sets S, S' connected by a simple permutation $v_{ijk,\sigma} \in \tilde{\mathcal{G}}$, we can choose a path of local automaton gates $u \in \mathcal{G}$ that implements a sequence of SWAPs to bring qubits i, j, k to consecutive positions (this takes $O(N)$ gates), implement the permutation σ (this takes $O(1)$ gates), and then return the three qubits to positions i, j, k ($O(N)$ gates again). In all this path has length $|\gamma_{S,S'}| \leq O(N)$. \square

Fact F.4. For any edge $e \in E$ we have

$$\sum_{S,S': \gamma_{S,S'} \ni e} \tilde{\Gamma}_{S,S'} \leq O(N). \quad (\text{F10})$$

Proof. We can write S' as $v(S)$ for some gate $v \in \tilde{\mathcal{G}}$. There may be more than one way to do this; to account for it, we introduce the multiplicity $\mu_{S,S'} \equiv |\{v \in \tilde{\mathcal{G}} : S' = v(S)\}|$. We obtain

$$\sum_{\substack{S,S' \in \Sigma_m: \\ \gamma_{S,S'} \ni e}} \tilde{\Gamma}_{S,S'} = \sum_{\substack{v \in \tilde{\mathcal{G}}: \\ \gamma_{S,v(S)} \ni e}} \frac{\tilde{\Gamma}_{S,v(S)}}{\mu_{S,v(S)}} \quad (\text{F11})$$

where the factor $1/\mu_{S,v(S)}$ accounts for the over-counting of terms when switching summation variables from S' to v . Now, by definition $\tilde{\Gamma}_{S,S'} = \mu_{S,S'}/|\tilde{\mathcal{G}}|$ (fraction of the gate set that maps S to S'), which gives

$$\sum_{\substack{S,S' \in \Sigma_m: \\ \gamma_{S,S'} \ni e}} \tilde{\Gamma}_{S,S'} = \frac{1}{|\tilde{\mathcal{G}}|} |\{(v, S) : \gamma_{S,v(S)} \ni e\}|. \quad (\text{F12})$$

Our choice of paths $\gamma_{S,S'}$ (see proof of Eq. (F9) above) depends only on the gate v (or more precisely, on one of the $\mu_{S,S'}$ possible gates that map S to $v(S)$, chosen arbitrarily): we decompose $v = u_l u_{l-1} \cdots u_1$ into a sequence of $l \leq O(N)$ local automaton gates, $u_i \in \mathcal{G}$. The condition $\gamma_{S,v(S)} \ni e$ thus requires that $e_1 = u_i \cdots u_1(S)$ and $e_2 = u_{i+1}(e_1)$ for some $i \in [l]$; equivalently, it requires $S = u_1 \cdots u_i(e_1)$. Therefore, given e and v , there are $O(N)$ choices for S , indexed by the integer i . The $|\tilde{\mathcal{G}}|$ choices for v cancel out the denominator in Eq. (F12), and we obtain the desired bound. \square

Putting it all together, Fact F.1 bounds the relaxation time in the ‘simple permutation’ Markov chain as $\tilde{t}_{\text{rel}}^{(m)} \leq O(mN^2)$; Facts F.2, F.3, and F.4 together yield the comparison coefficient $B \leq O(N^3)$; plugging these into the comparison bound (Eq. (F2)) gives the desired result (Eq. (F4)).

We close with two observations. First, since our best lower bound on the mixing time (for general m) is $t_{\text{mix}}^{(m)} \geq \tilde{\Omega}(mN)$, this upper bound on $t_{\text{rel}}^{(m)}$ is not sufficient to separate the relaxation and mixing times. Second, using the relaxation time, we can also bound the mixing time above by Eq. 28. This gives the (likely loose) upper bound $t_{\text{mix}}^{(m)} \leq O(m^2 N^6)$.

Appendix G: Upper bound on pseudothermalization time for subset states

In this Appendix we prove the upper bound Eq. (44) on the pseudothermalization time for subset states, Sec. V. We start from the key result, Eq. (38-39), which relates pseudothermalization to the equilibration of the Markov chains $\Phi_{m+\delta \leftarrow K}[p_t]$ on $\Sigma_{m+\delta}$, for $\delta = 0, \dots, m$.

Let us decompose the matrix $\mathcal{M}_{p_t}^{(m)}$ based on the values of the difference between subsets, $\delta = |S' \setminus S''|$:

$$\mathcal{M}_{p_t}^{(m)} = \sum_{\delta=0}^m O_\delta, \quad (\text{G1})$$

$$O_\delta = \binom{K}{m}^{-1} \binom{K}{m+\delta} \times \sum_{\substack{S', S'' \in \Sigma_m: \\ |S' \setminus S''| = \delta}} |S'\rangle f_{p_t}^{(m+\delta)}(S' \cup S'') \langle S''|, \quad (\text{G2})$$

where $f_{p_t}^{(m+\delta)}$ is defined in Eq. (40). The diagonal term O_0 provides a lower bound: $\|\mathcal{M}_{p_t}^{(m)}\| \geq \|O_0\|$, which is used to derive the lower bound on the prethermalization time, Eq. (43). To get an upper bound, we need to consider the off-diagonal terms as well.

We have

$$\|\mathcal{M}_{p_t}^{(m)}\|_{\text{tr}} \leq \sum_{\delta=0}^m \|O_\delta\|_{\text{tr}}. \quad (\text{G3})$$

We will upper-bound each $\|O_\delta\|_{\text{tr}}$ by the sum of the absolute values of its elements: for any operator A , one has

$$\|A\|_{\text{tr}} = \left\| \sum_{ij} A_{ij} |i\rangle\langle j| \right\|_{\text{tr}} \leq \sum_{ij} \|A_{ij} |i\rangle\langle j|\|_{\text{tr}} = \sum_{ij} |A_{ij}|. \quad (\text{G4})$$

For each δ , the set of possible entries is given by $f_{m+\delta}(S)$, with $S \in \Sigma_{m+\delta}$. Each entry appears multiple times: there are $\binom{m+\delta}{m} \binom{m}{m-\delta}$ ways of choosing $S', S'' \in \Sigma_m$ such that $|S' \cup S''| = m + \delta$. Therefore,

$$\begin{aligned}
\|O_\delta\|_{\text{tr}} &\leq \sum_{S \in \Sigma_{m+\delta}} \binom{m+\delta}{m} \binom{m}{m-\delta} \binom{K}{m}^{-1} \binom{K}{m+\delta} |f_{p_t}^{(m+\delta)}(S)| \\
&\leq \binom{m}{\delta} \binom{K-m}{\delta} \sum_{S \in \Sigma_{m+\delta}} |\Phi_{m+\delta \leftarrow K}[p_t](S) - \pi_{m+\delta}(S)| \\
&= \binom{m}{\delta} \binom{K-m}{\delta} \Delta_{m+\delta},
\end{aligned} \tag{G5}$$

where in the second line we combined the various binomial coefficients and in the last line we recognized the total variation distance:

$$\Delta_{m+\delta} = \|\Phi_{m+\delta \leftarrow K}[p_t] - \pi_{m+\delta}\|_{\text{tv}}. \tag{G6}$$

Now, using the results of Appendix B, and specifically Fact B.4, we have that $\Delta_{m+\delta}$ is non-decreasing in δ . It follows that

$$\|\mathcal{M}_{p_t}^{(m)}\|_{\text{tr}} \leq \Delta_{2m} \sum_{\delta=0}^m \binom{m}{\delta} \binom{K-m}{\delta} = \binom{K}{m} \Delta_{2m}. \tag{G7}$$

Thus, to make the LHS smaller than ϵ , the Markov chain on Σ_{2m} must equilibrate to within total variation error $\Delta_{2m} \leq \binom{K}{m}^{-1} \epsilon$. Defining the mixing time $t_{\text{mix}}(\epsilon)$ based on a total variation threshold ϵ (see Sec. IIB), one has the following general inequality:

$$t_{\text{mix}}(2^{-l-1}) \leq l t_{\text{mix}}(1/4). \tag{G8}$$

It follows then that

$$t_{\text{PTerm}}^{(m)} \leq \left[\log_2 \binom{K}{m} \right] t_{\text{mix}}^{(2m)} \leq m \log_2(K) t_{\text{mix}}^{(2m)}. \tag{G9}$$

Finally, invoking the upper bound on the mixing time (conditional on Conjecture 1) gives

$$t_{\text{PTerm}}^{(m)} \leq O(\log(K) m^2 N^2). \tag{G10}$$

In the case of $K = \exp(\text{polylog}(N))$ (where the entropy of the random subset ensemble is polylogarithmic) this reduces to

$$t_{\text{PTerm}}^{(m)} \leq \tilde{O}(m^2 N^2), \tag{G11}$$

where the symbol \tilde{O} represents an upper bound up to $\log(N)$ factors.